

Modeling Neuron Material Transport Using Isogeometric Analysis, Deep Learning and PDE- constrained Optimization

Angran Li

Co-workers: Yongjie Jessica Zhang, Ge Yang, Xiaoqi Chai

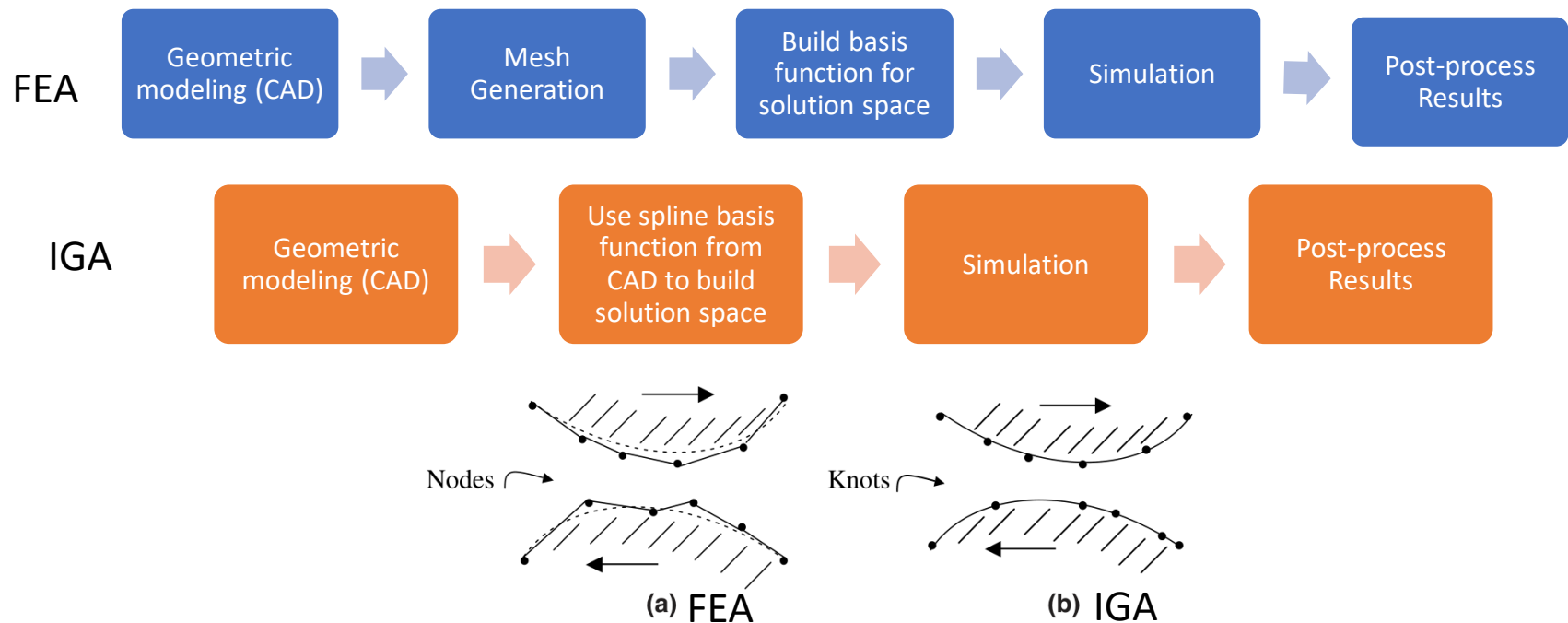
Sep 28, 2022

Overview

1. Introduction
2. IGA-based Material Transport Simulation In Complex Geometry of Neurons
3. GNN-based Deep Learning Model of Material Transport In Complex Neurite Networks
4. Modeling Material Transport Regulation and Traffic Jam In Neurons Using PDE-constrained Optimization
5. Conclusion and Future Work

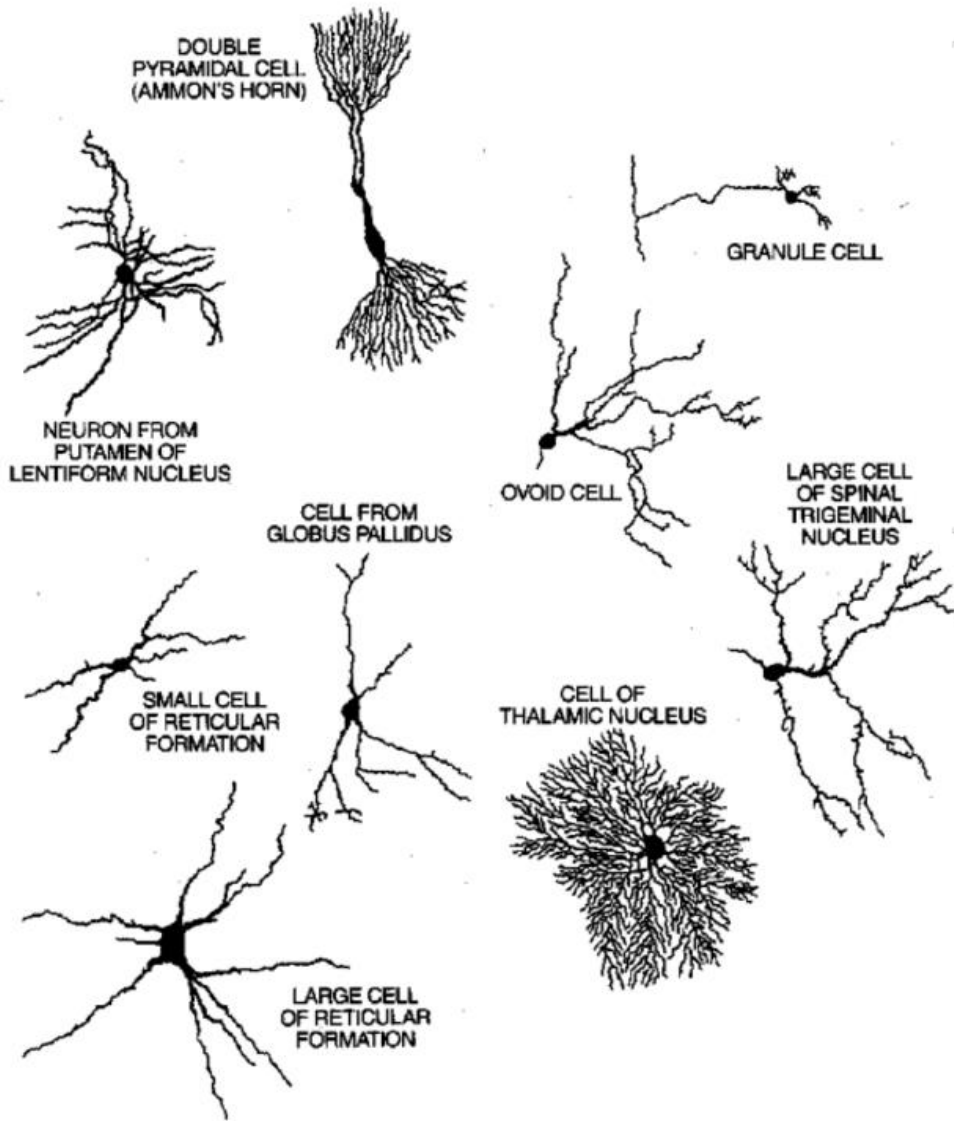
Introduction Isogeometric Analysis

- Isogeometric analysis (IGA) is a variant of traditional finite element analysis (FEA) that **integrates Computer Aided Design (CAD) with traditional FEA**.
- Compared to FEA, IGA uses the same smooth spline basis functions for geometrical modeling and numerical solution. Thus, IGA can preserve the exact geometry with less degree of freedoms.

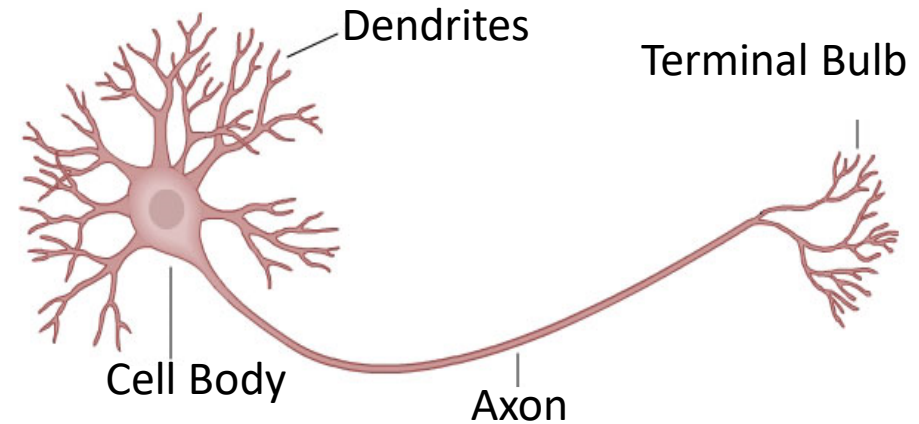


Introduction

- Overview of neuron geometry



— A Typical Neuron —

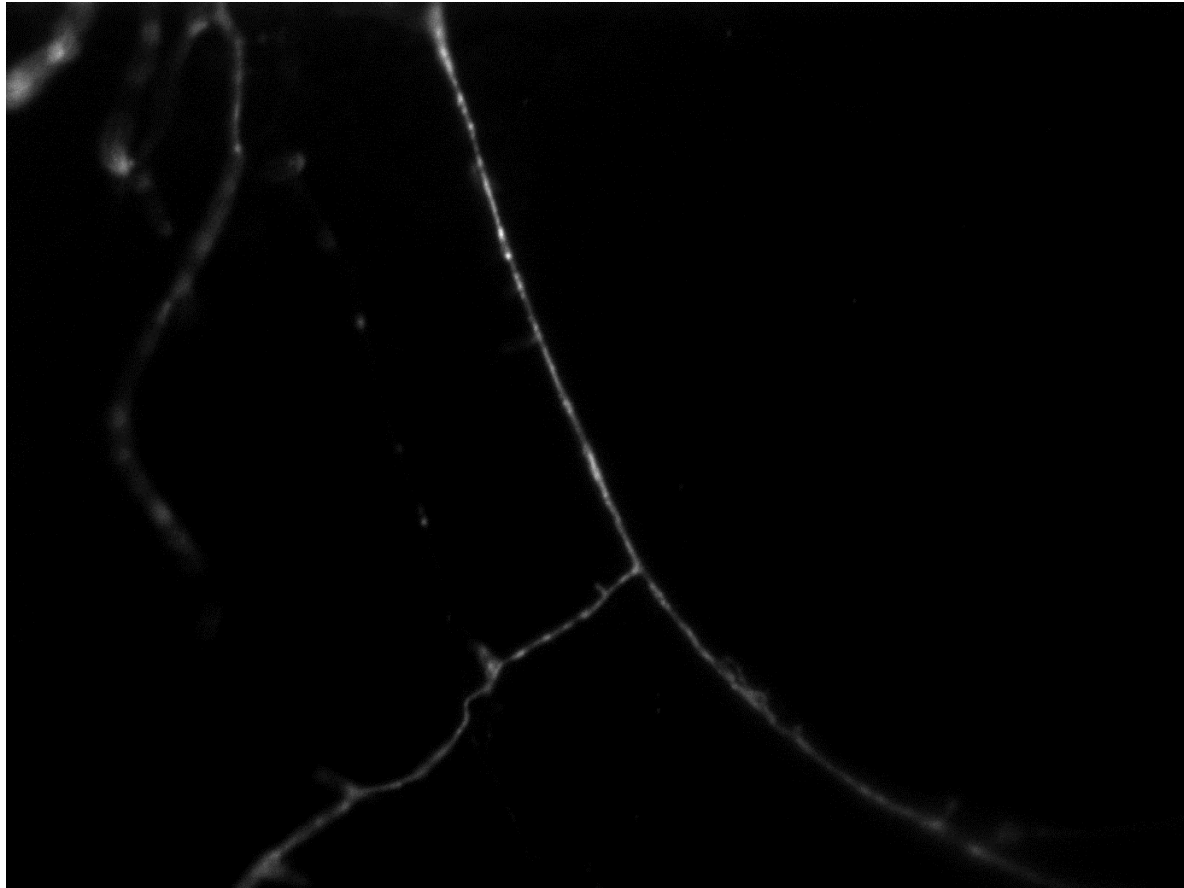


Typical neuron structure

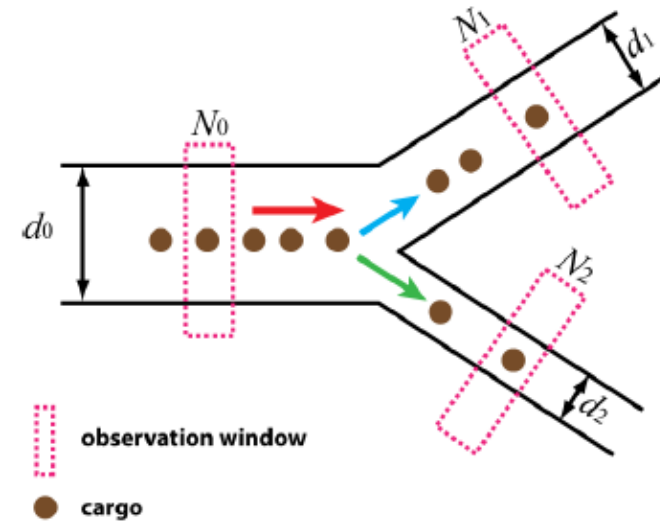
The complexity of the geometry causes a significant transportation challenge because material synthesis and degradation in neurons are carried out mainly in the cell body.

Introduction

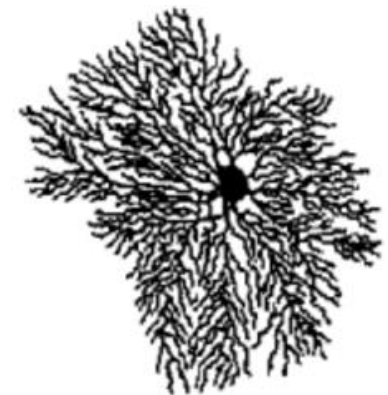
- Material transport in neuron



The transport of synaptic vesicles over a branch



Analyzing traffic routing at neurite junction

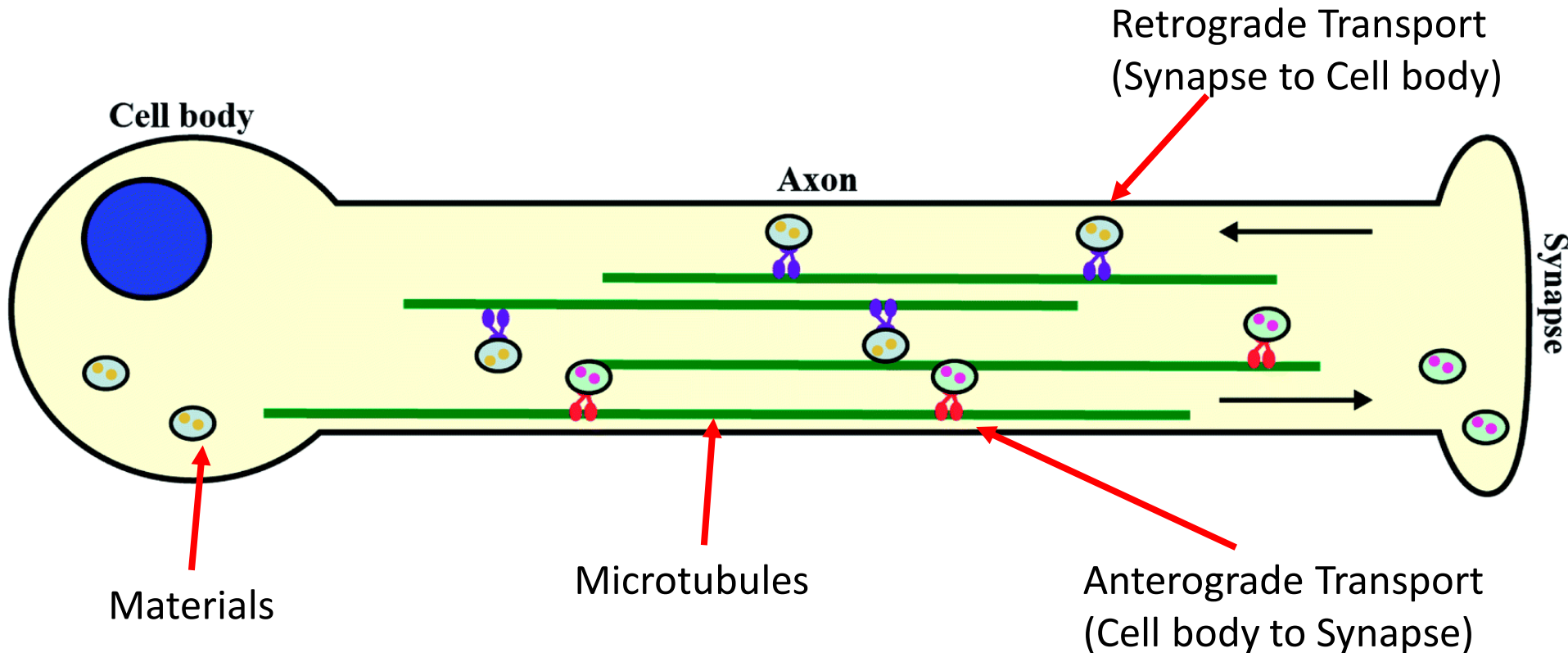


- **Objective: Study the traffic control of material transport in neurons**

IGA-based Material Transport Simulation In Complex Geometry of Neurons

Background

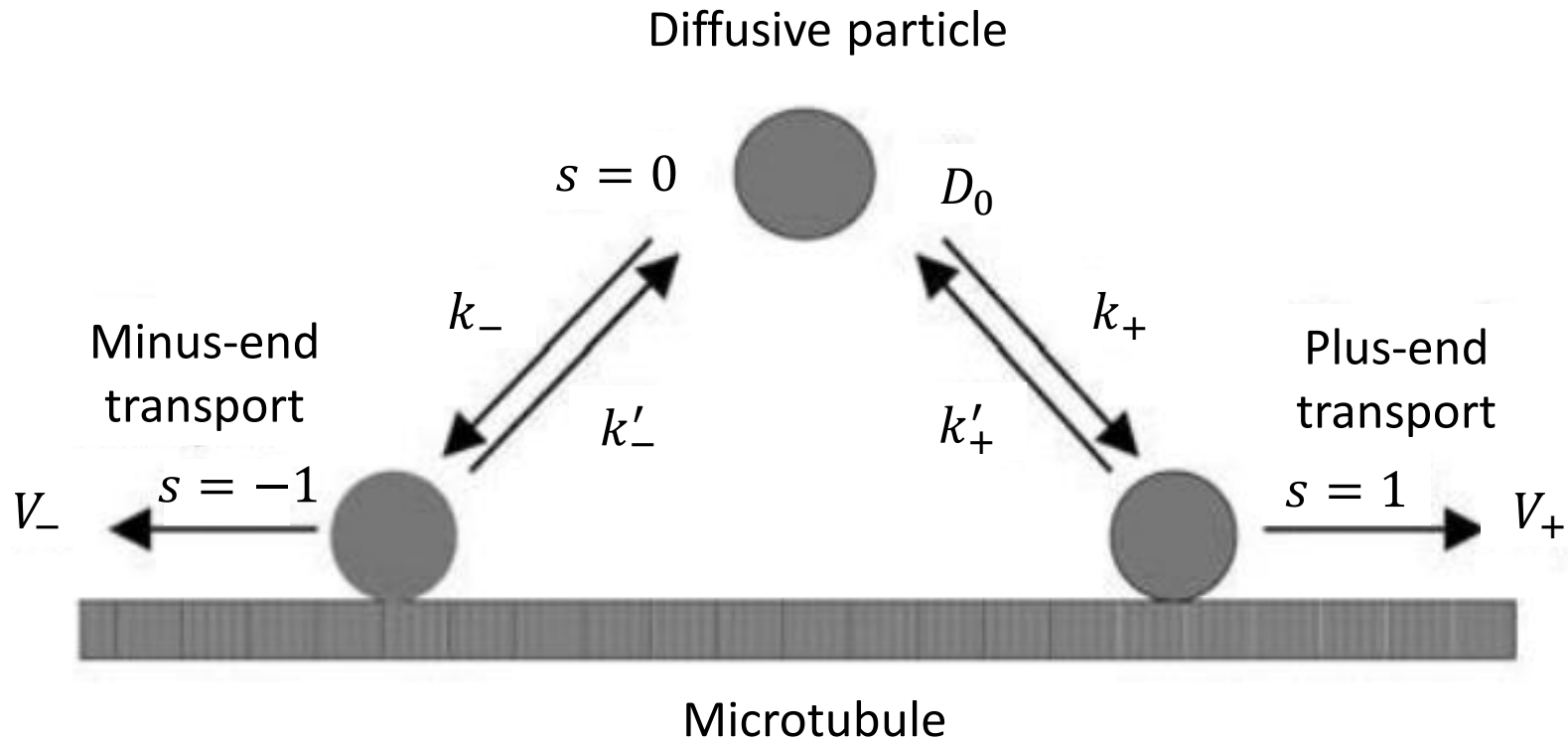
- Molecular motors and mechanisms of directional transport in neurons



Rohena, C. C., & Mooberry, S. L. (2014). Recent progress with microtubule stabilizers: new compounds, binding modes and cellular activities. *Natural product reports*, 31(3), 335-355.

Background

- Motor-assisted transport model [1]

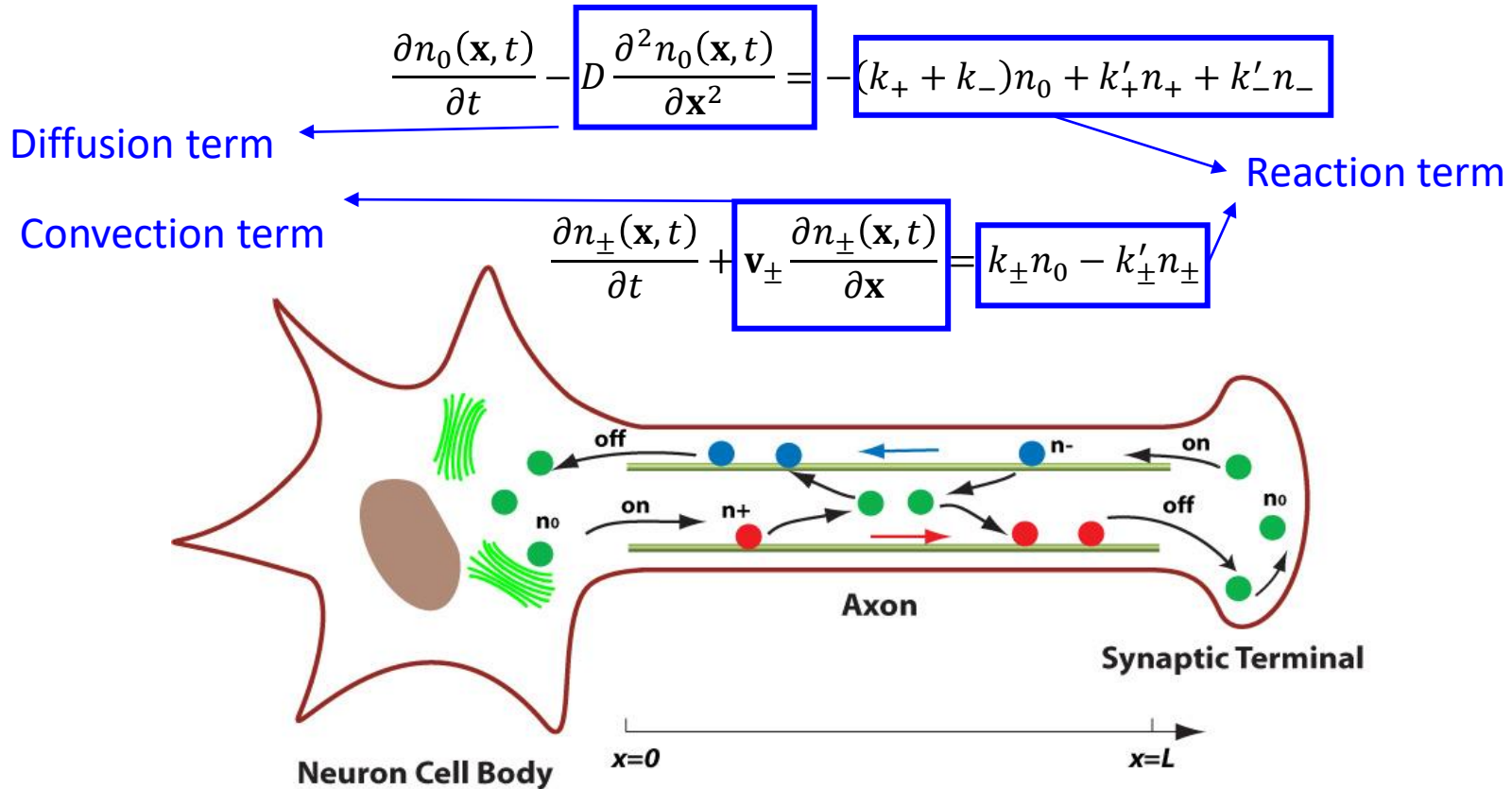


Transition map of between transport states [2]

- Study the transport using a PDE model in **1D domain**.
- Method: **Finite Difference Method (FDM)**

Model of Material Transport

- We model the transport of material in neurite network by generalizing the motor-assisted transport model to 3D domain:



- To get the velocity field, we solve the steady incompressible Navier-Stokes Equation and couple with the motor-assisted transport model:

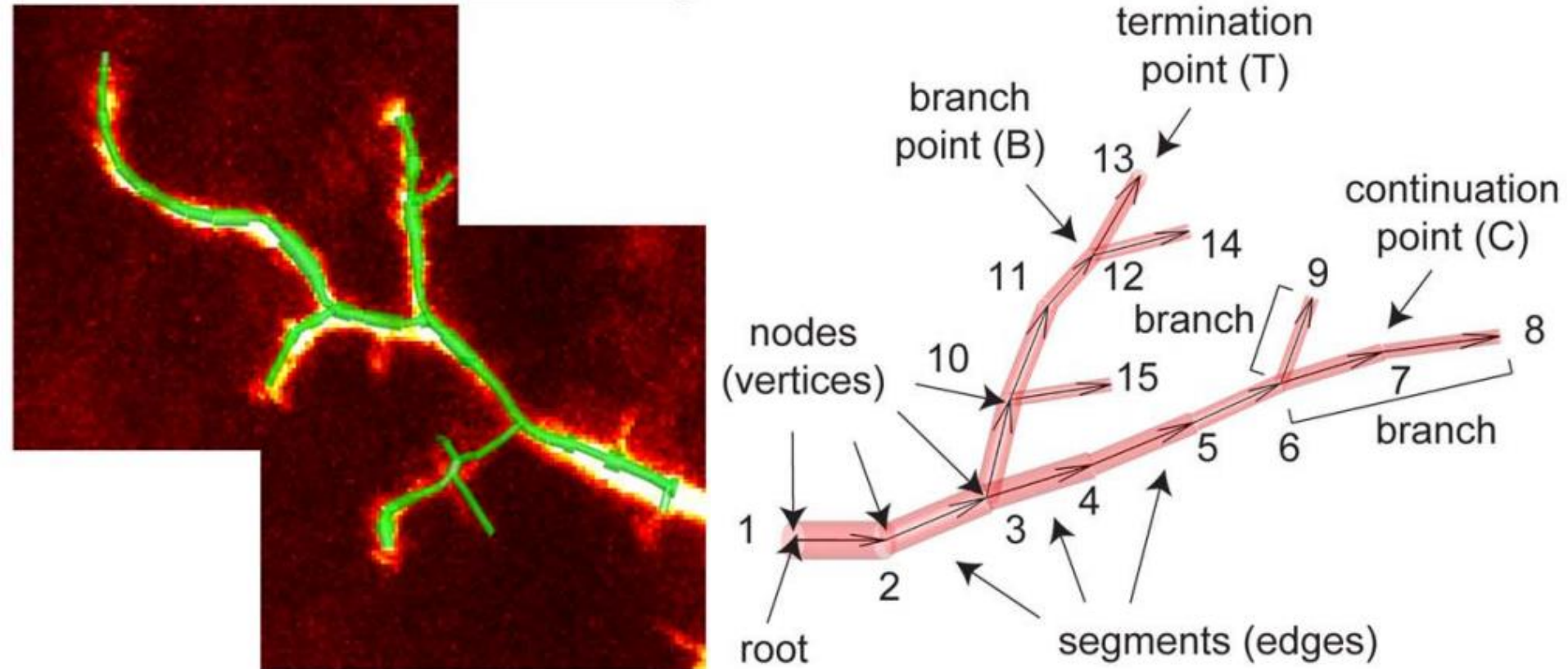
$$\nabla \cdot \mathbf{u} = 0$$

$$\nabla \cdot (\mathbf{u} \otimes \mathbf{u}) + \nabla p = \nu \Delta \mathbf{u} + \mathbf{f}$$

Tree structure reconstruction

- Matlab–TREES toolbox

The toolbox can reconstruct geometry of neurons by an input 'swc' file.

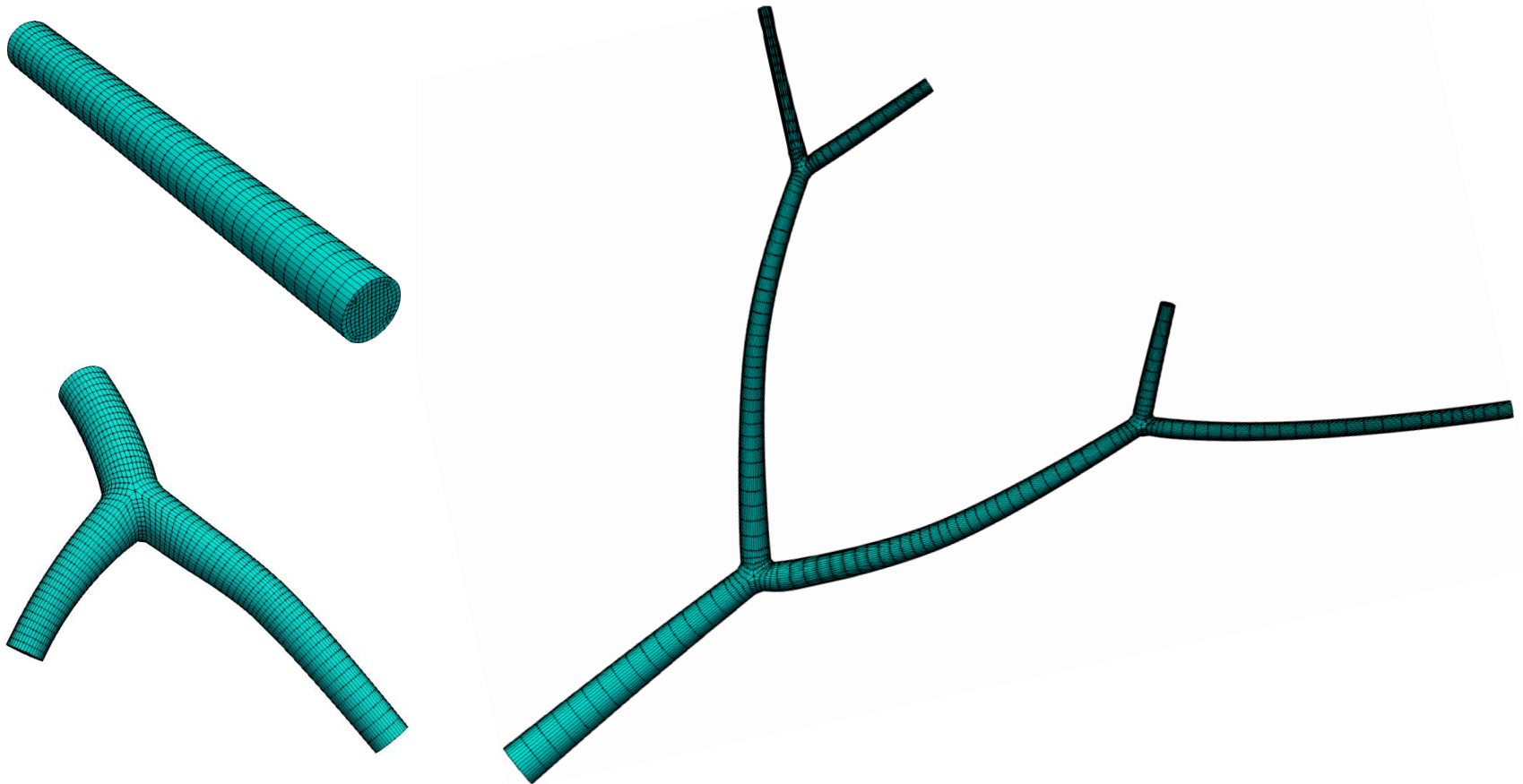


Example of TREES toolbox

Method for mesh generation

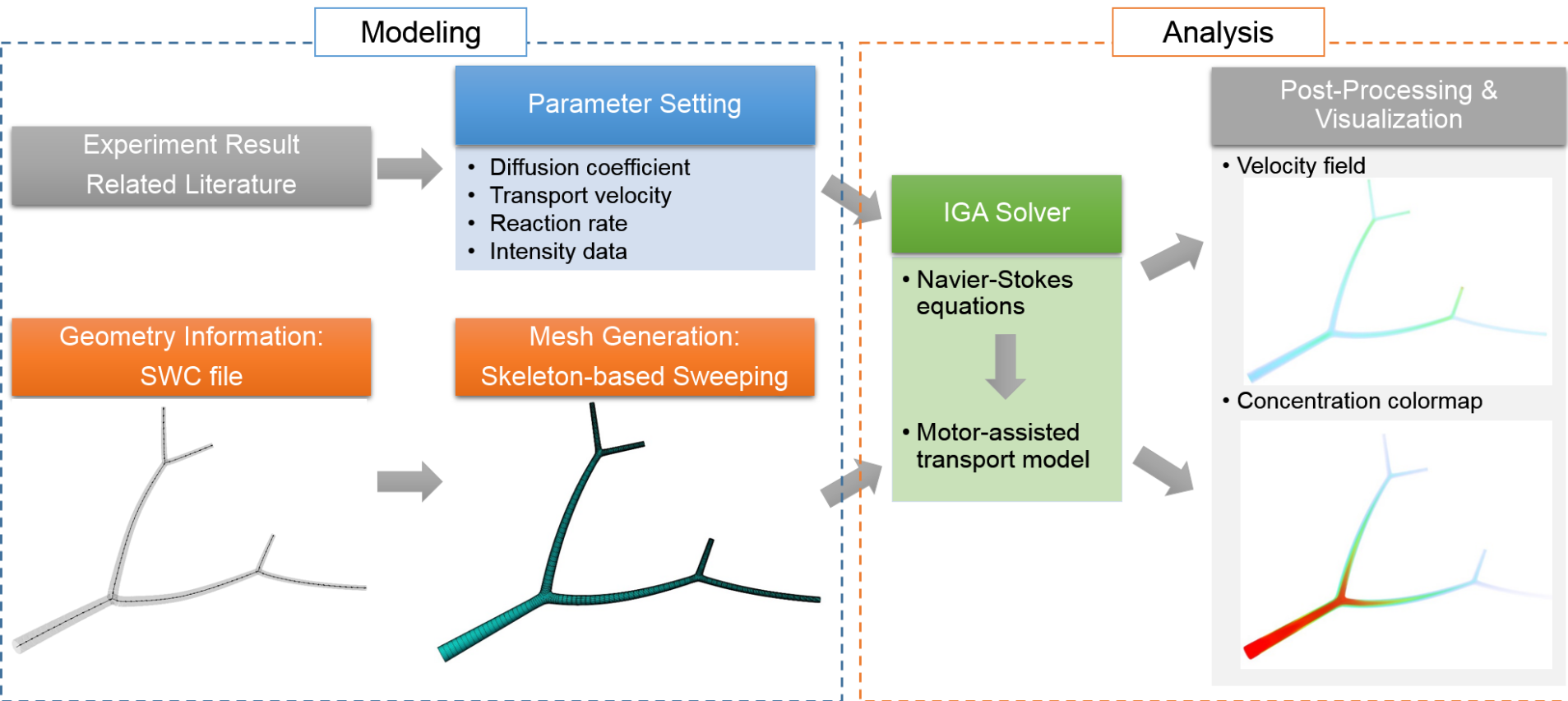
- Skeleton-based sweeping method

Basic idea: sweep the cross-section template along the neuron skeleton



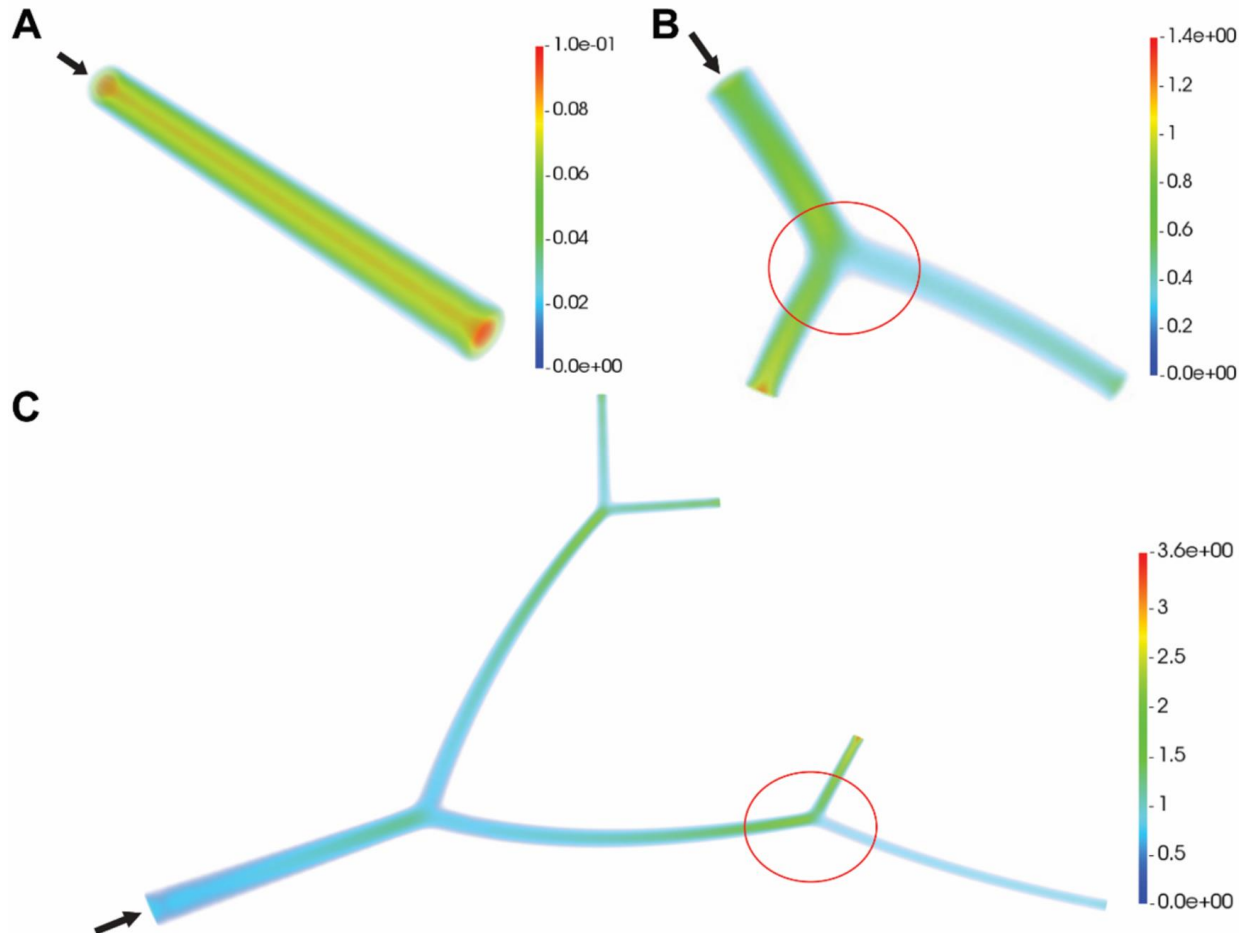
Mesh generation examples for some simple neuron geometries

Simulation Pipeline Summary



Result in three simple neurons: Velocity

- Problem setting:
 - Unidirectional transport
 - Parabolic inlet velocity

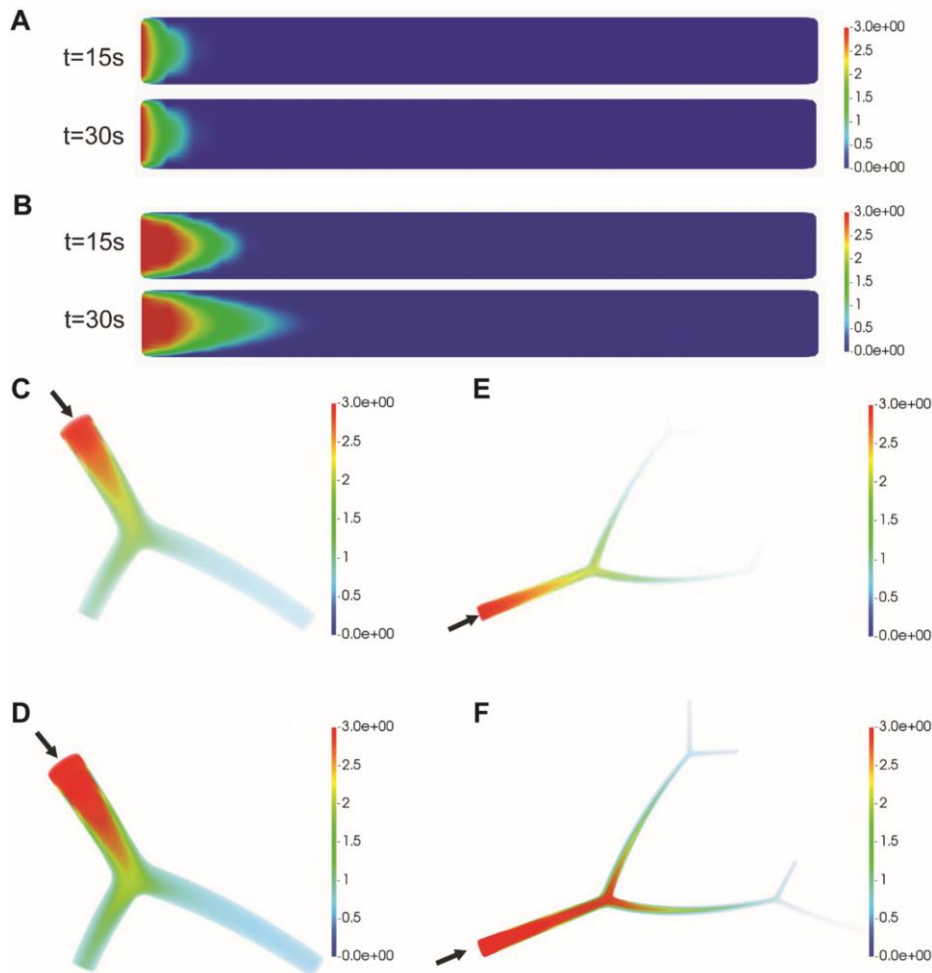


- Sudden increase in the velocity magnitude is observed near the branching point in both bifurcation models (red circle regions).
- The velocity magnitude is higher in shorter branch.

Result in three simple neurons: Concentration

We compare the concentration results with different detachment rates:

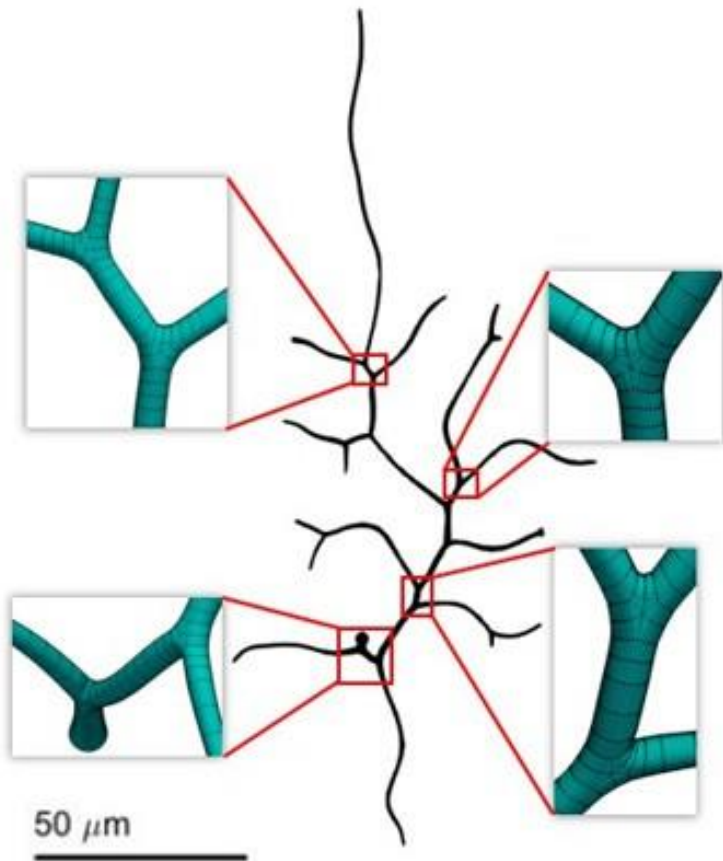
- $k' = 0.5 s^{-1}$ (Fig. A, C, E)
- $k' = 0.1 s^{-1}$ (Fig. B, D, F)



- The propagation is faster under the lower detachment rate.
- For the one-bifurcation model (Fig. C&D), transport exhibits faster propagation in the left branch than in the right branch. Similar observation is obtained in the neurite tree of three bifurcations (Fig. E&F)

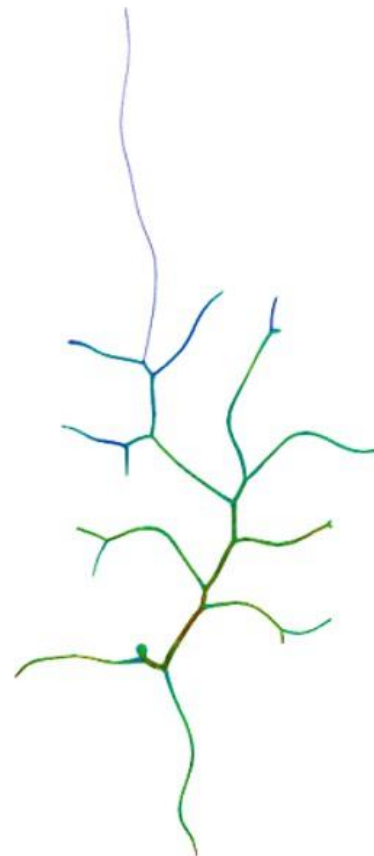
Conclusion: Geometry affects the velocity field inside neurites and in turn affects the spatial distribution of transported material.

Result for Complex Neurite Network

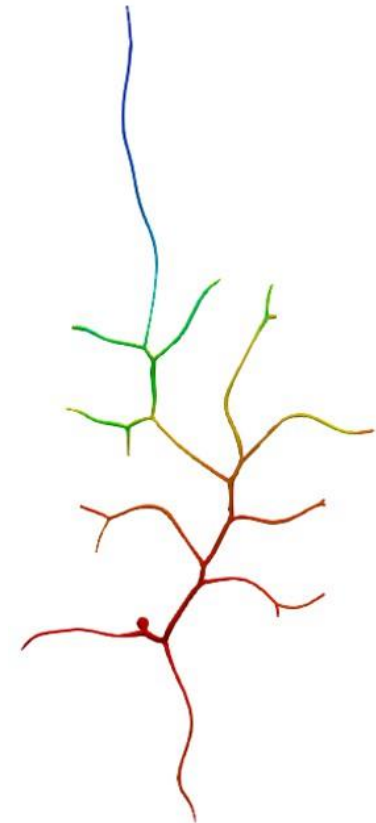
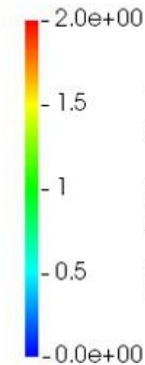


Geometry and mesh for Neuron
NMO_66731:

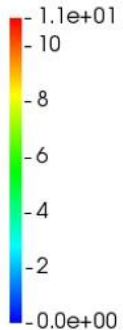
A zebrafish retina neuron
(Data comes from the
NeuroMorpho database)



Velocity field

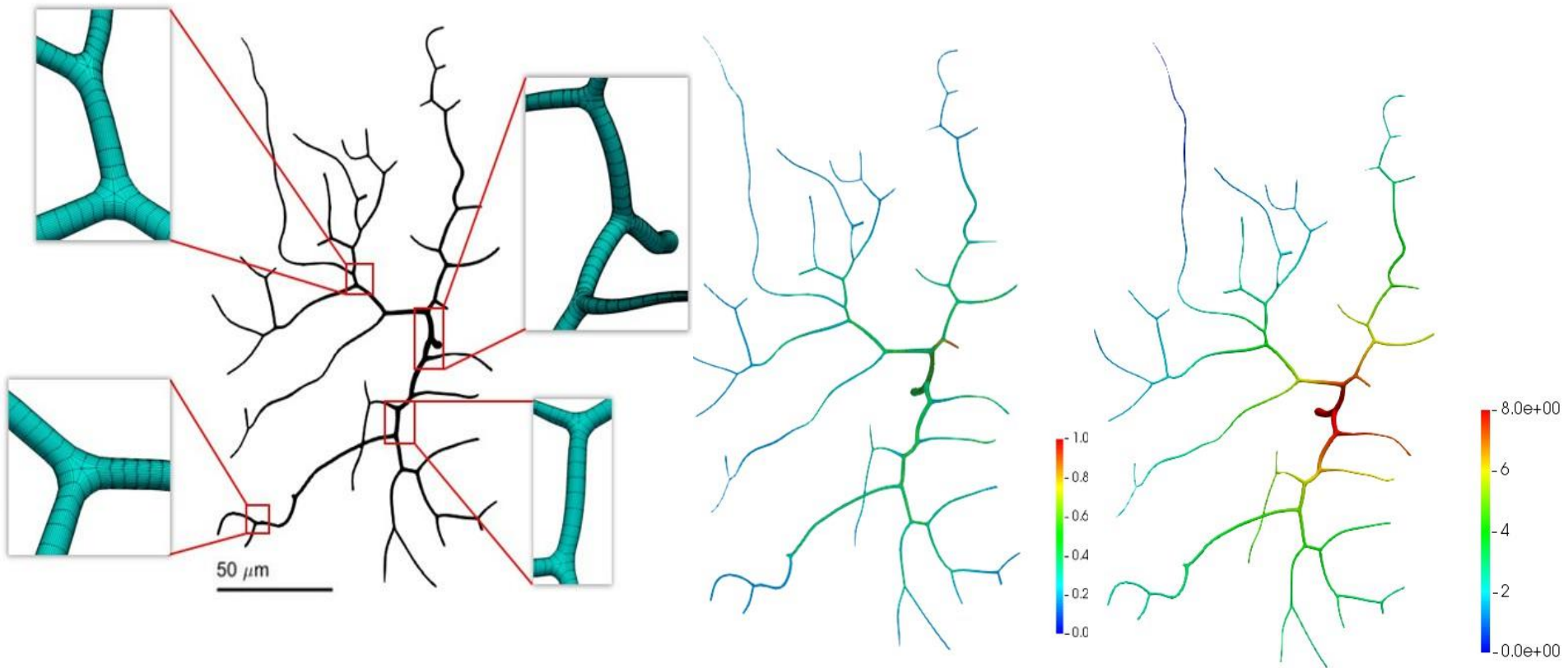


Concentration colormap



The material is prior to transport to high velocity region.

Result for Complex Neurite Network



Geometry and mesh for Neuron

NMO_66748:

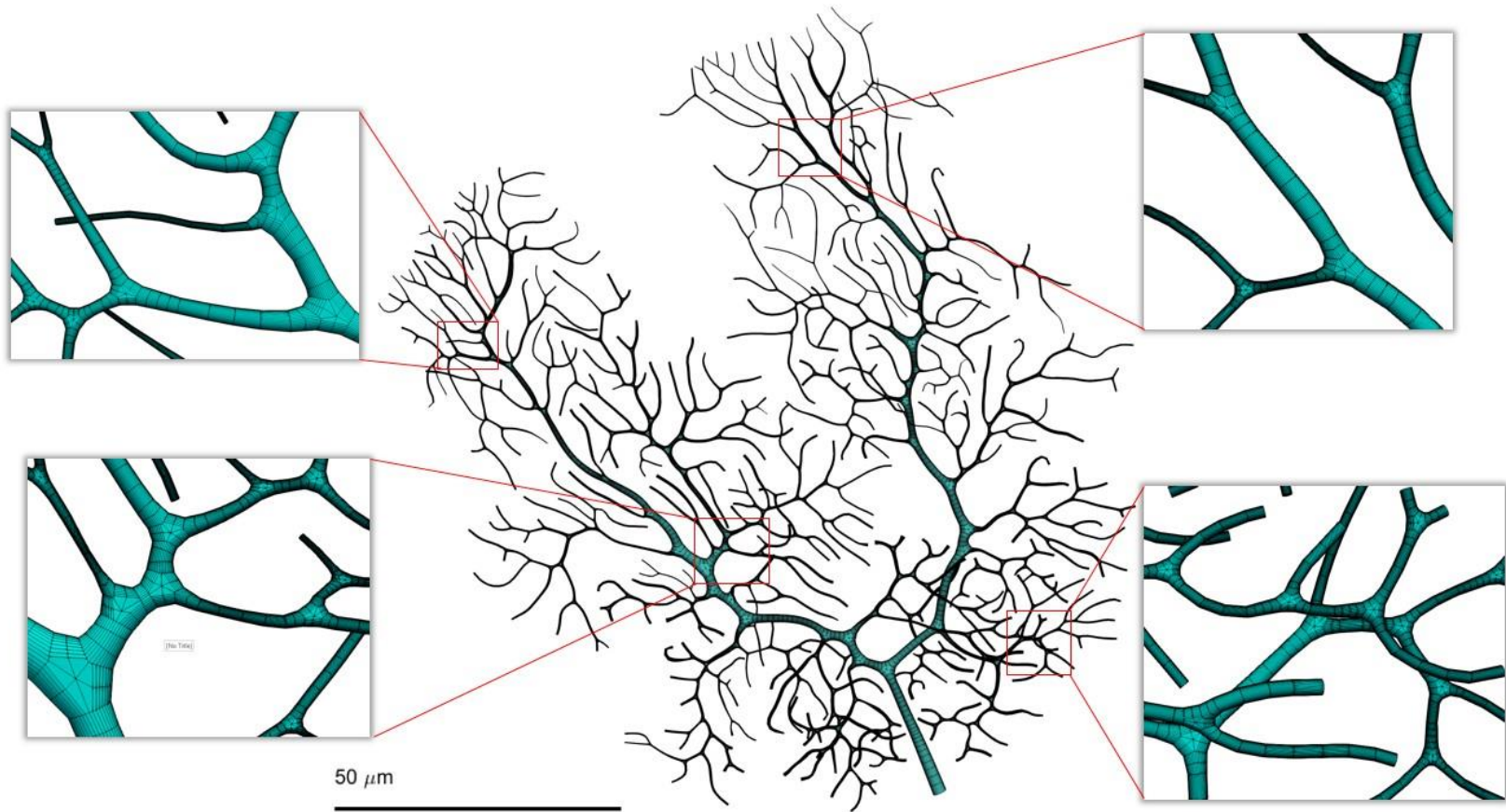
A zebrafish retina neuron
(Data comes from the
NeuroMorpho database)

Velocity field

Concentration colormap

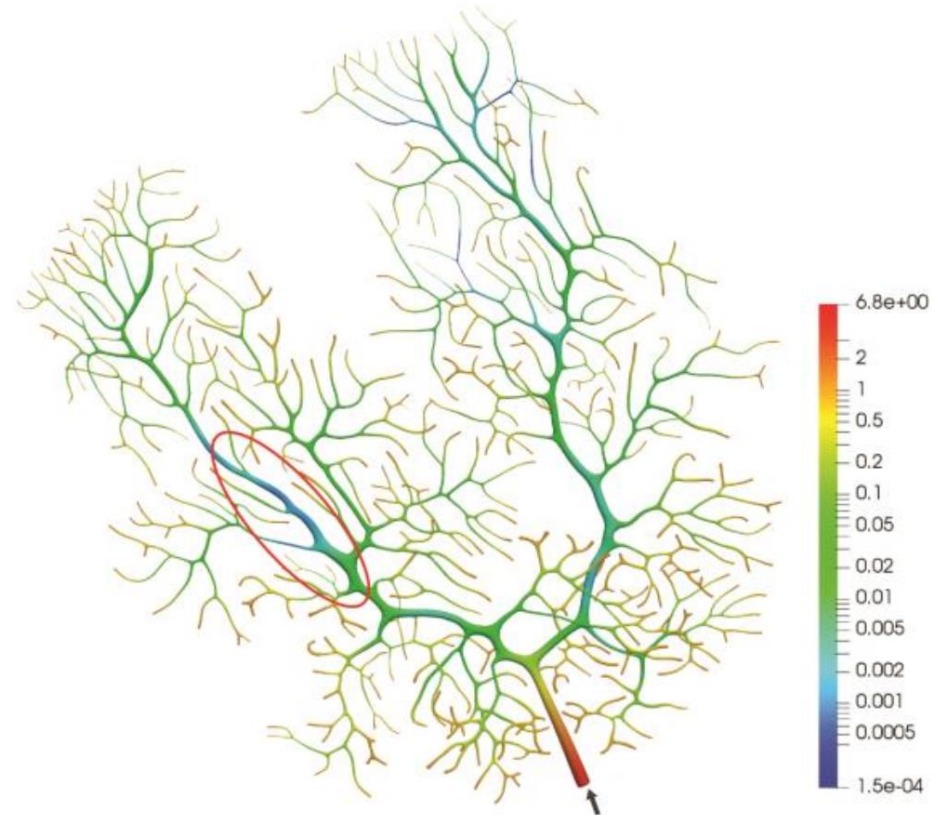
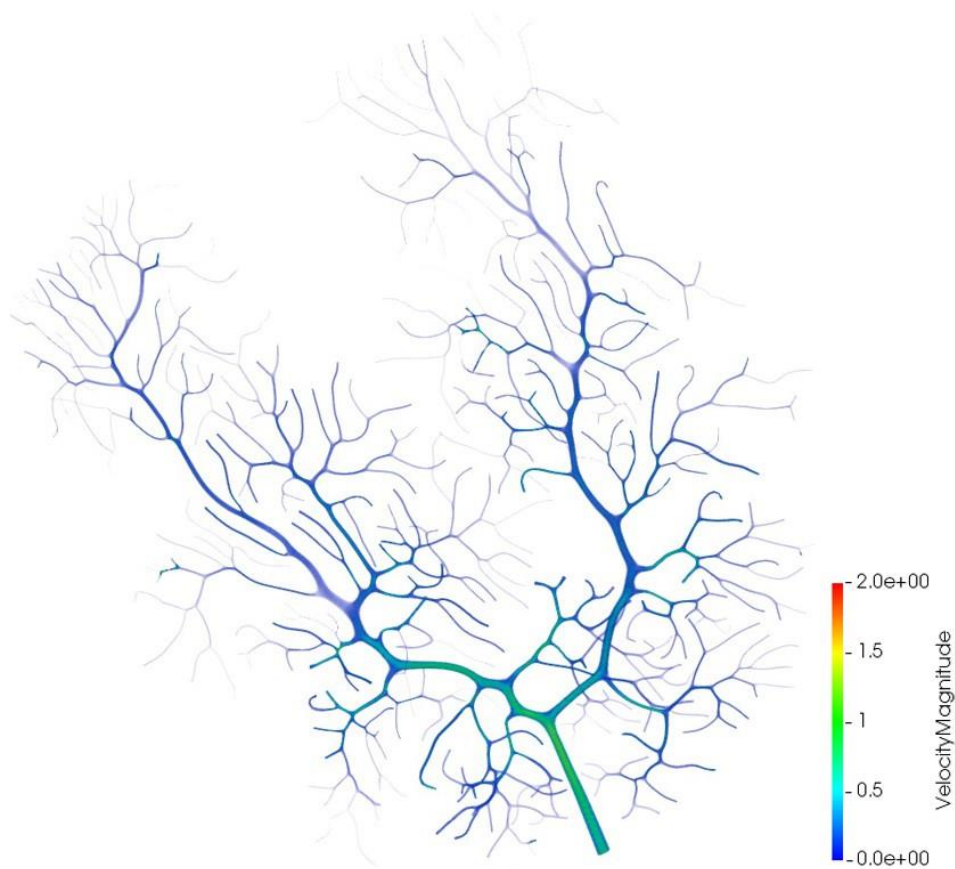
The transport priority is not obvious for more complex geometry.

Result for Complex Neurite Network

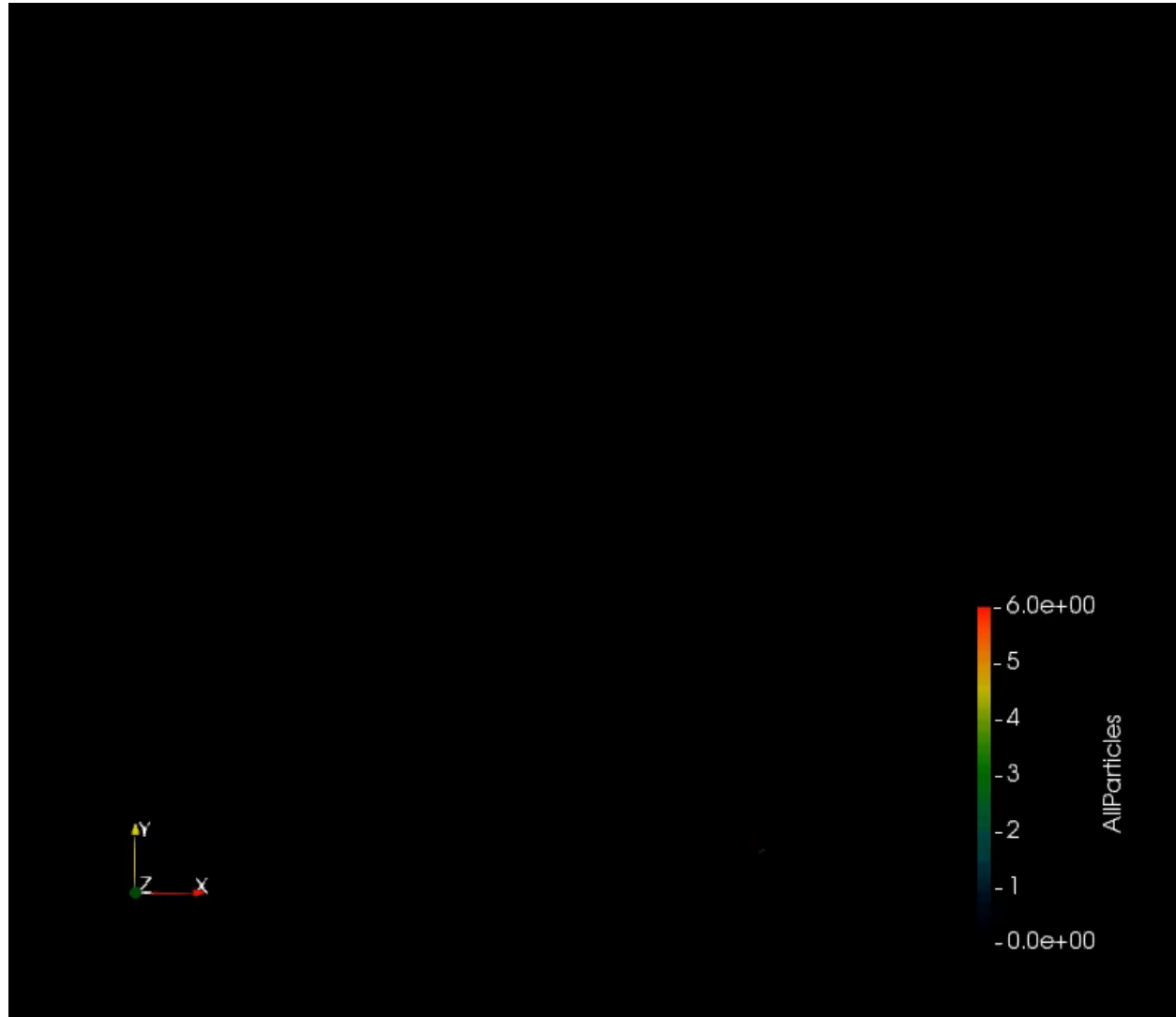


Geometry and mesh for Neuron NMO_00865
 A mouse cerebellum Purkinje neuron
 (Data comes from the NeuroMorpho database)

Result for Complex Neurite Network



Result for Complex Neurite Network



The simulation result in a mouse cerebellum Purkinje neuron showing the dynamic material transport process for 350 seconds. The colormap represents the concentration of the material.

Summary

- An IGA-based computational platform to study cellular process in neuron

The solver can provide the concentration prediction of material transport process for complex neuron geometry. It can also be extended to solve other PDE models of cellular processes in complex neurite network geometry.

- The transport process is mediated by neuron geometry

Our results show how the complex network geometry mediates spatial patterns of transport velocities at neurite junctions and within different branches. The spatial patterns of transport velocities in turn drive different distributions of transported material in different regions of neurite networks.

GNN-based Deep Learning Model of Material Transport In Complex Neurite Networks

Motivation

- The “Big data” generated by material transport simulation includes massive velocity and concentration information that can be used to study the transport mechanism and material spatial pattern in neuron.
- The computational cost of the simulation is too expensive, and we need a surrogate to provide faster prediction result.

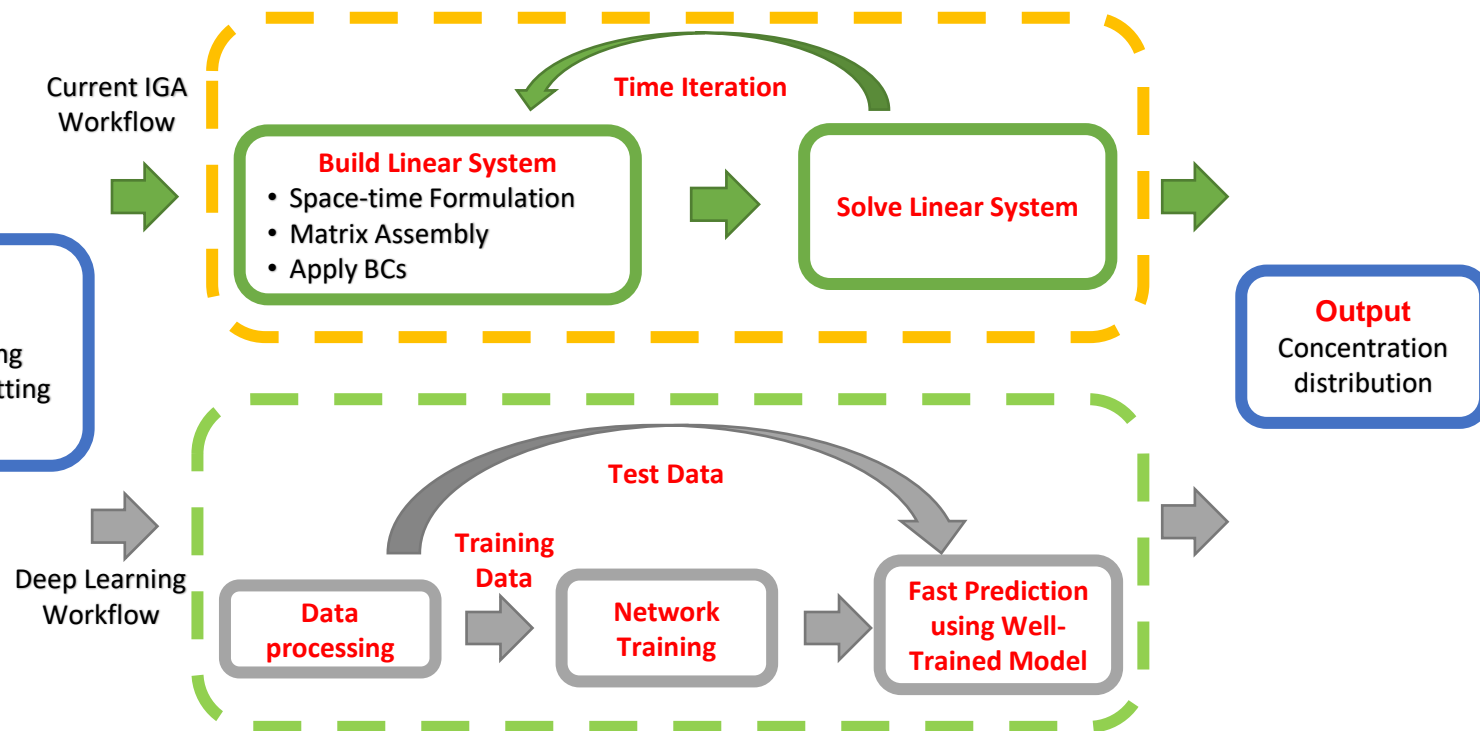


Figure: A comparison between IGA and deep learning workflow

Challenge

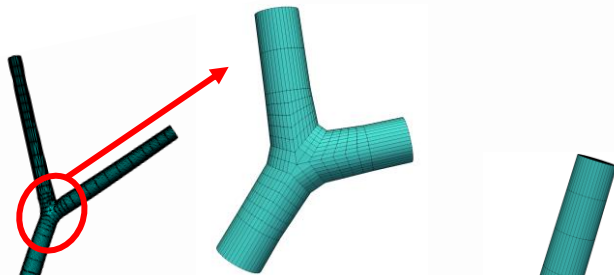
- **The sample data from simulation is stored in unstructured mesh**
Current deep learning technique like convolutional neural network (CNN) is mature to handle the data stored in structured quadrilateral or hexahedral mesh. How to efficiently handle unstructured data format is still an emerging problem in machine learning field.
- **Extensive neuron geometries with different topologies**
The deep learning model needs to be trained with the geometry information encoded as input feature to fit for any complex geometry.

Graph neural network (GNN) could be a solution for these problems, since it can directly handle non-Euclidean 3D representations like point clouds, graphs, and meshes.

Graph representation of neuron geometry

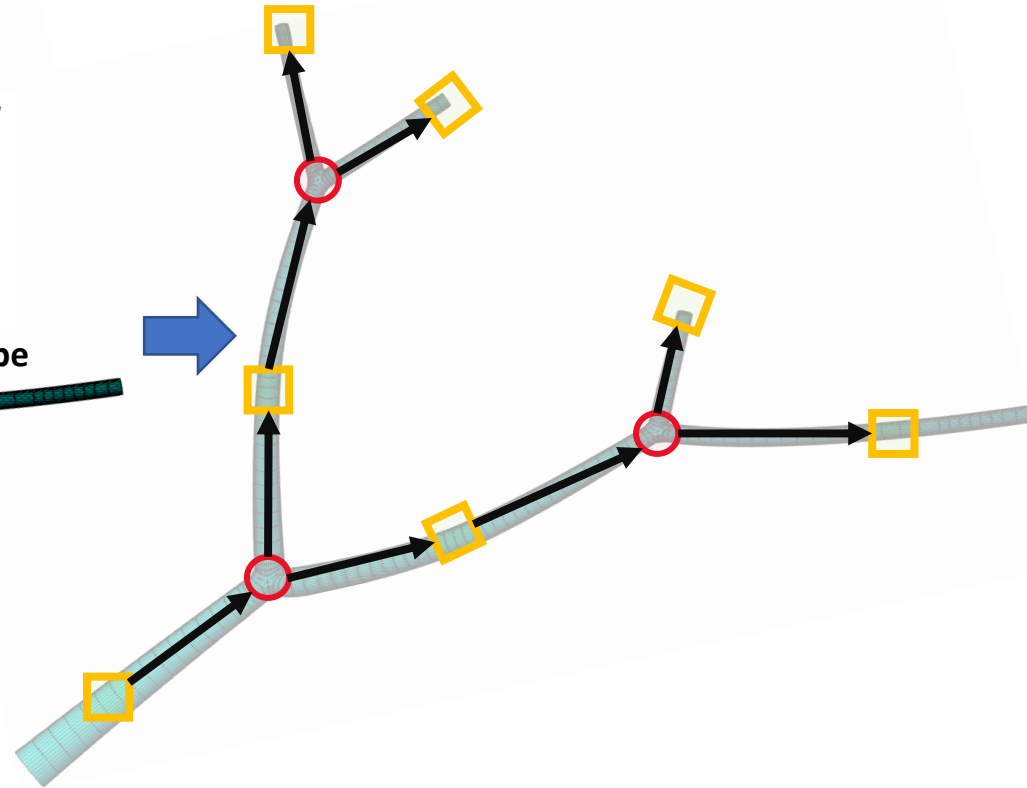
- For each neuron tree, the geometry can be decomposed into two basic units

Bifurcation



Single pipe

- The neuron tree can be represented as a graph. The nodes represent the decomposed bifurcations and single pipes. The directed edges show the skeleton of the tree.



Input neuron geometry

Output neuron graph

GNN Framework

Our GNN model is built on the graph representation, and it consists of two parts:

- The simulator for bifurcation (F_b) and pipe (F_p)

$$x^{k+1/2} = F_{b \text{ or } p}(x^k, c_i, c_b, v_p)$$

Input: Prediction value x^k from step k , initial condition c_i , boundary condition c_b , simulation parameters v_p .

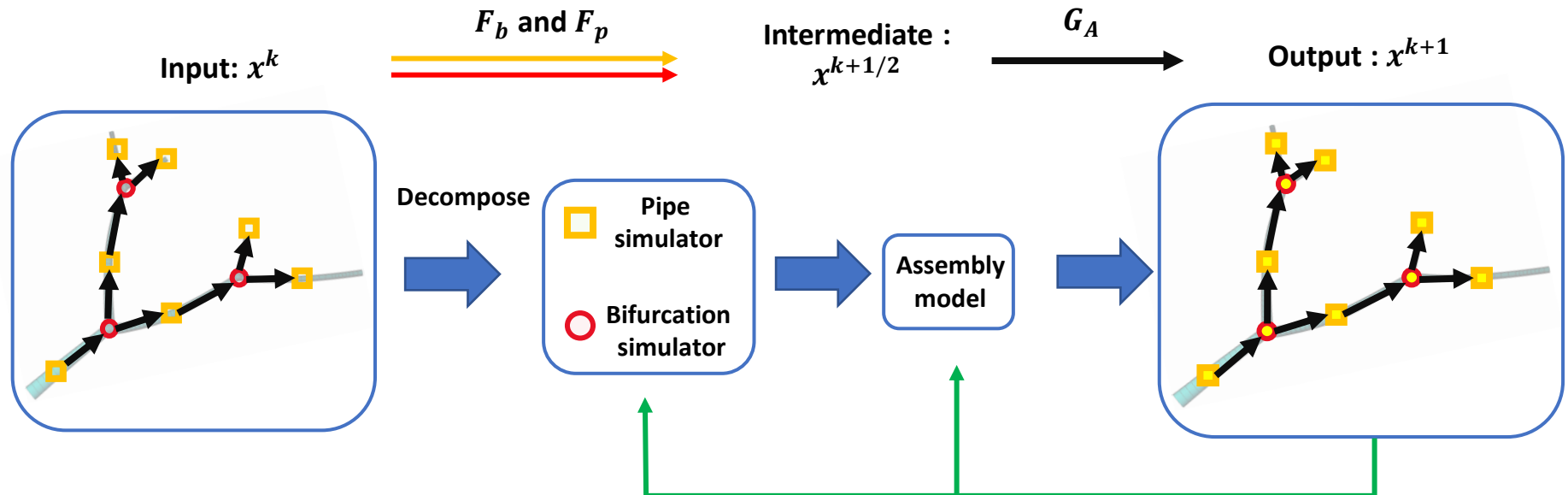
Output: Prediction value $x^{k+1/2}$ before assembly.

- The assembly model (G_A):

$$x^{k+1} = G_A(x^{k+1/2}, c_i, c_b, v_p)$$

Input: Prediction value $x^{k+1/2}$ from simulator, initial condition c_i , boundary condition c_b , simulation parameters v_p .

Output: Prediction value x^{k+1} after assembly.



Training process: compare with target concentration values and update parameters in simulator and assembly model

Figure: GNN framework

GNN Simulator for local prediction in pipe and bifurcation

- Two different GNN simulators are trained for **pipe** and **bifurcation** structures.
- The GNN simulator adopts a recurrent “GN block + MLP Decoder” scheme.
- The loss function includes the residual term from PDEs:

$$\mathcal{L}_{simulator} = \frac{1}{N} \sum_{i=1}^N [(n_{0,i}^P - n_{0,i}^G)^2 + (n_{\pm,i}^P - n_{\pm,i}^G)^2] +$$

Mean square error

$$\frac{1}{N} \sum \left[\frac{\partial n_0}{\partial t} - D \nabla^2 n_0 + (k_+ + k_-) n_0 - k'_+ n_+ + k'_- n_- \right]^2 +$$

Residual term from PDE

$$\frac{1}{N} \sum \left[\frac{\partial n_{\pm}}{\partial t} + \mathbf{v}_{\pm} \cdot \nabla n_{\pm} - k_{\pm} n_0 + k'_{\pm} n_{\pm} \right]^2,$$

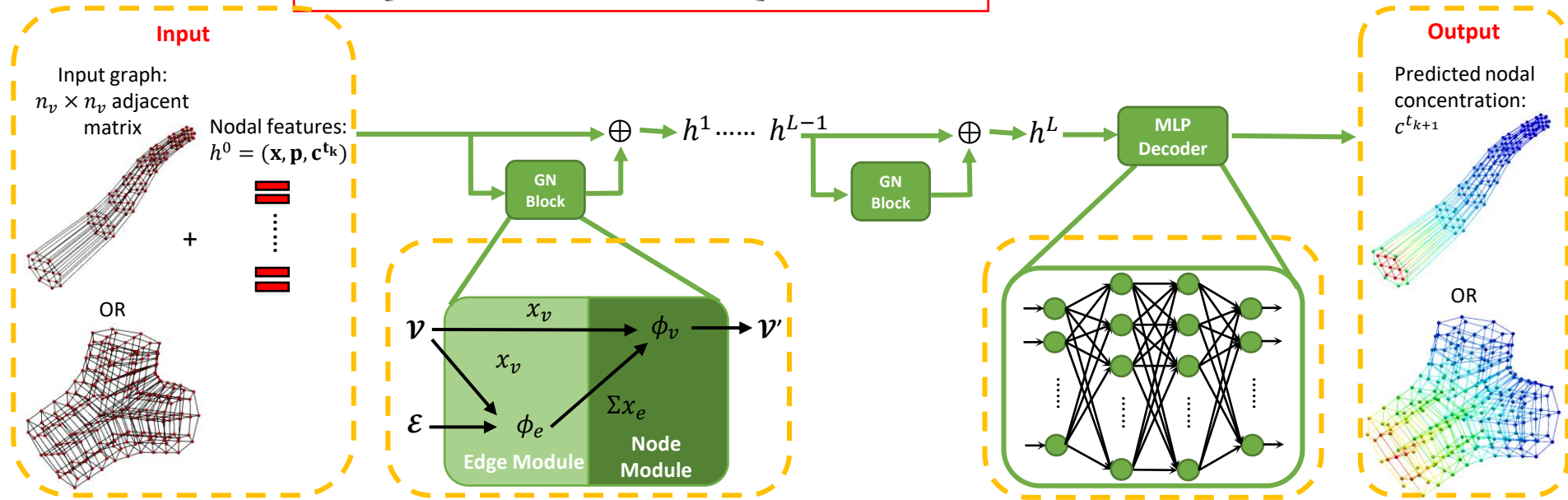


Figure: The architecture of GNN simulator

GNN assembly model to improve global prediction

- The GNN assembly accounts for three types of assembly during prediction
- The GNN assembly model gathers predicted information from its neighboring simulators
- The loss function includes a penalty term to ensure consistent results at assembly interface

$$\mathcal{L}_{assemble} = \frac{1}{N} \sum_{i=1}^N \left\{ (n_{0,i}^P - n_{0,i}^G)^2 + (n_{\pm,i}^P - n_{\pm,i}^G)^2 \right\} + \text{Mean square error}$$

$$\alpha \frac{1}{M} \sum_{i=1}^M \left\{ (n_{0,i}^{s_1,interface} - n_{0,i}^{s_2,interface})^2 + (n_{\pm,i}^{s_1,interface} - n_{\pm,i}^{s_2,interface})^2 \right\} \text{Penalty term to impose consistent prediction on interface}$$

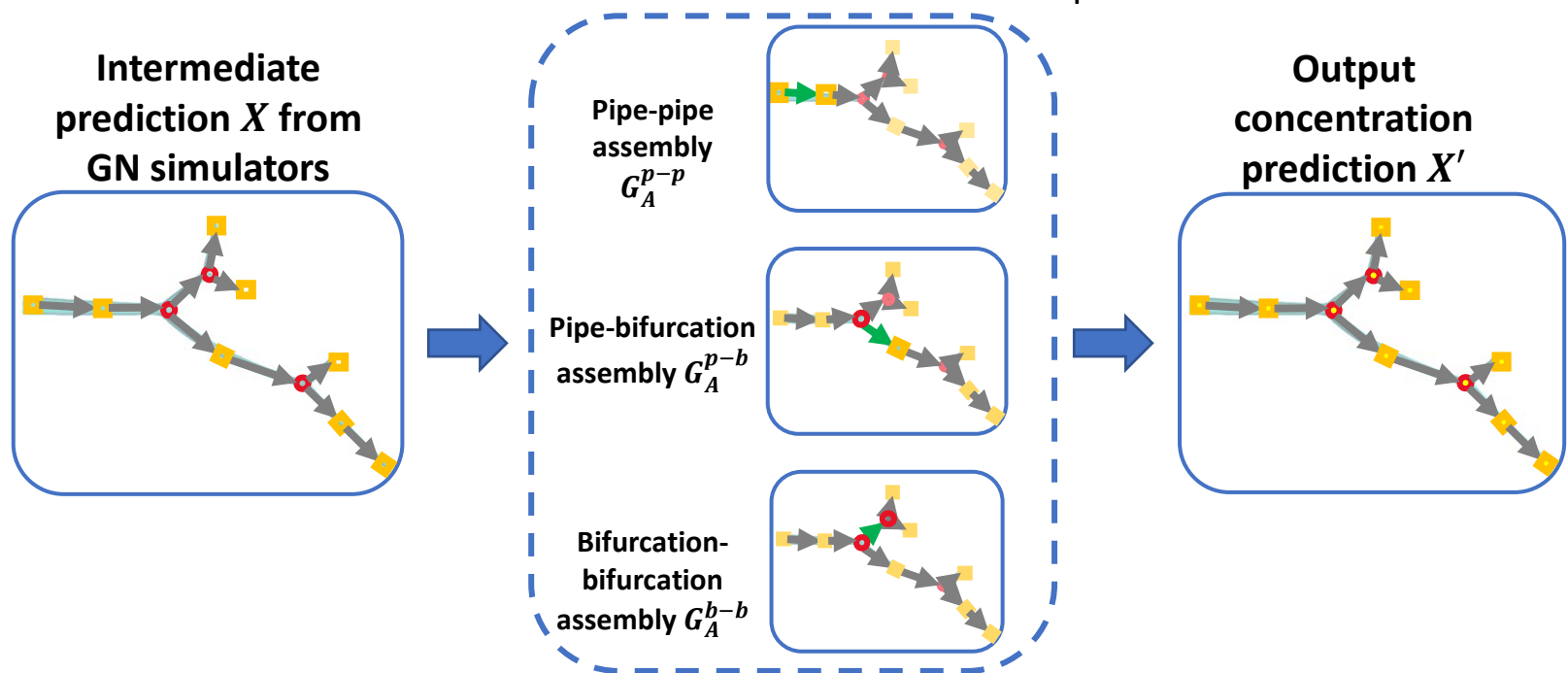


Figure: The architecture of GNN assembly model

Dataset generation and training

- We run IGA simulations in 2 different geometries and 200 different boundary conditions to collect data
 - Constant parameters are $D = 1.0 \frac{\mu m}{s^2}$, $k = 1.0 s^{-1}$, $k' = 0.5 s^{-1}$, $u_i = 0.1 \mu m/s$
 - For each simulator, extract 20,000 samples = 100 (pipes/bifurcations) * 200 (boundary conditions)
 - For each type of assembly, extract 30 different geometries
 - 75% samples used for training and 25% for testing
 - The performance is evaluated using mean relative error (MRE)

$$MRE = \frac{\sqrt{\sum_{i=1}^N \frac{1}{N} (c_i^P - c_i^G)^2}}{\max||c^G|| - \min||c^G||} \times 100\%$$

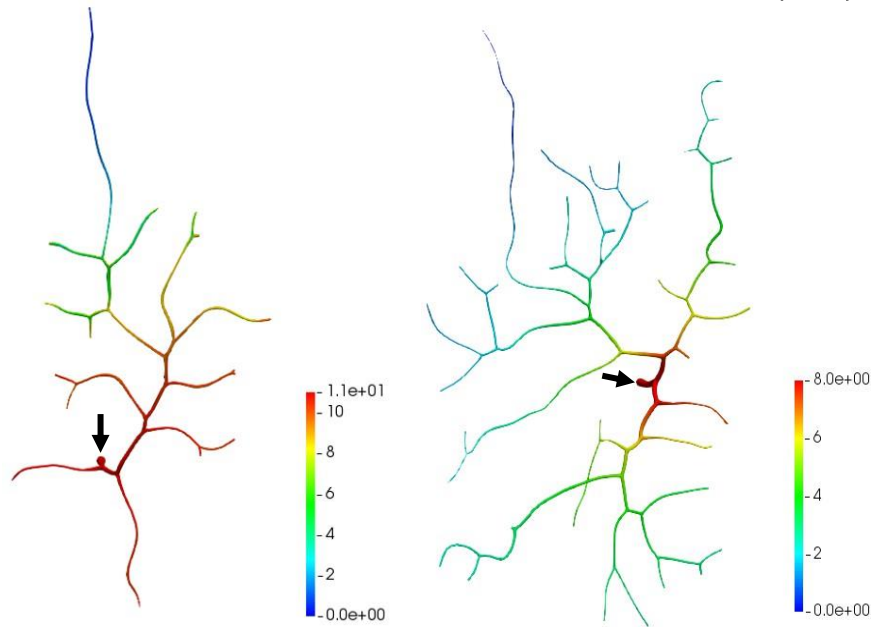


Figure 1: Two neuron geometries used for data generation: NMO_66731 (left), NMO_66748 (right)

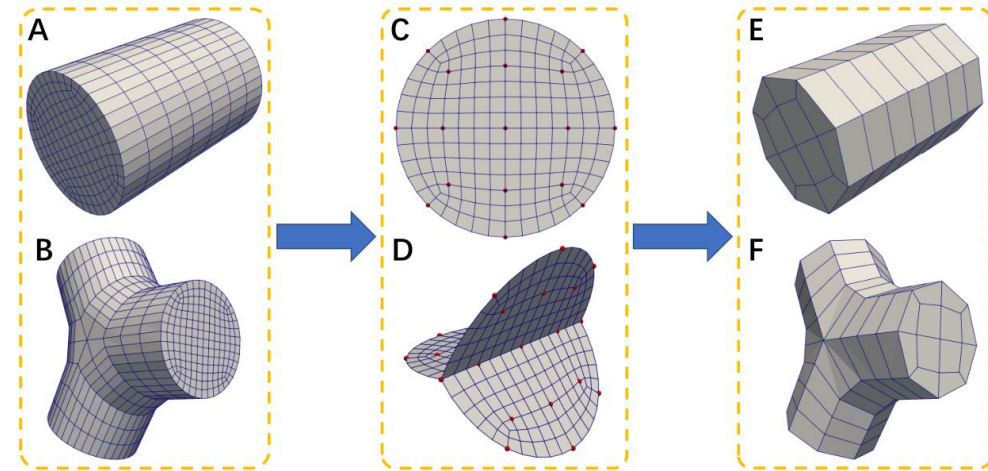


Figure 2: The graph extraction of the pipe and bifurcation structures

Results – prediction in complex neuron trees

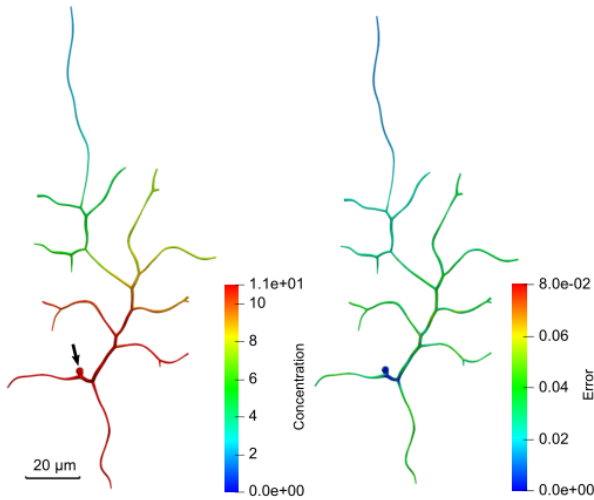


Figure 1: NMO_66731

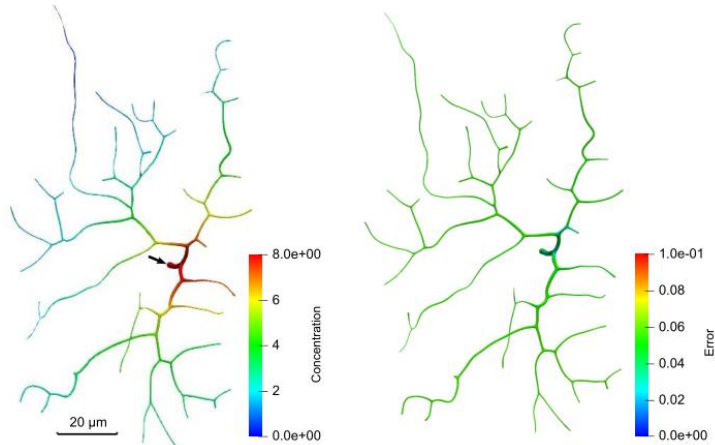


Figure 2: NMO_66748

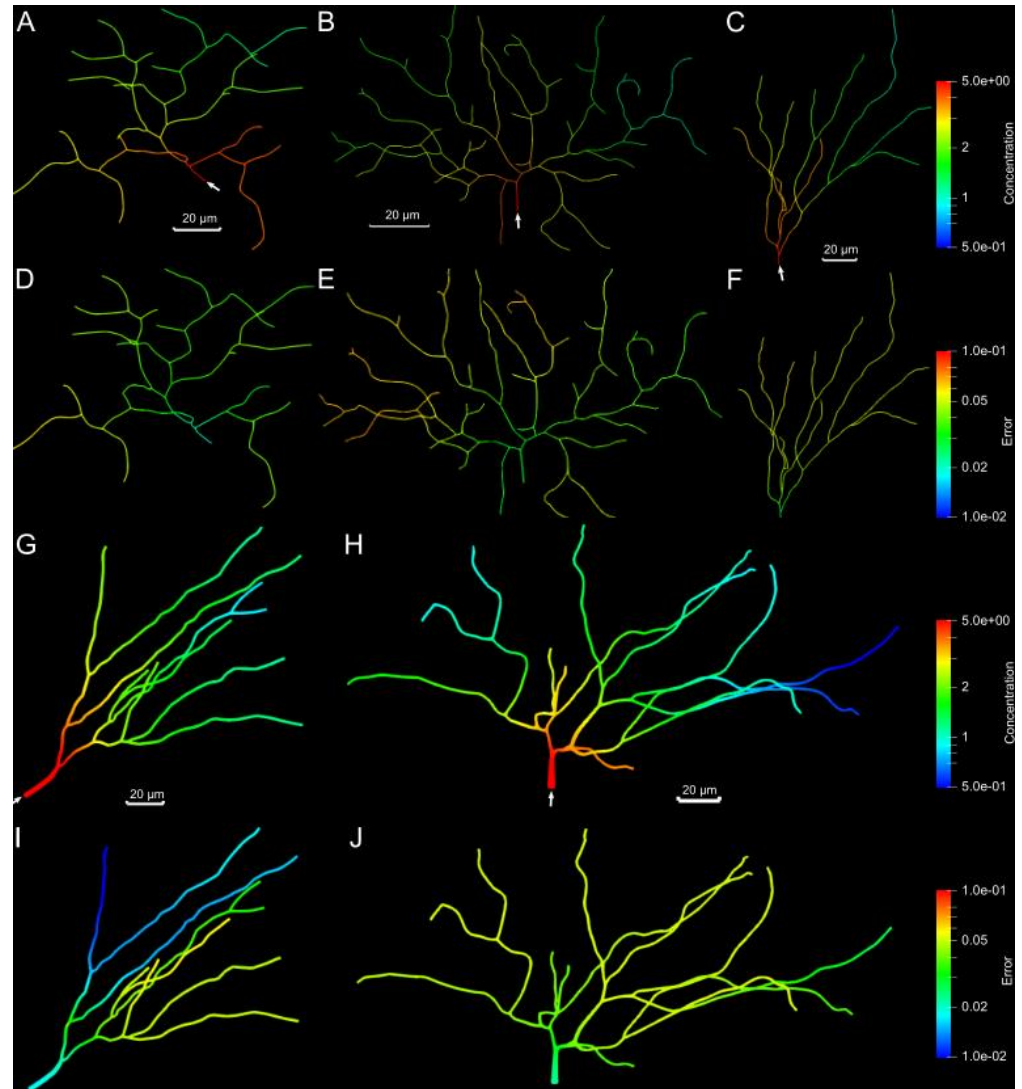


Figure 3: (A,D) NMO_06846; (B,E)NMO_06840;
(C,F)NMO_112145; (G,I)NMO_32235; (H,J)NMO_32280;

Results – prediction in complex neuron trees

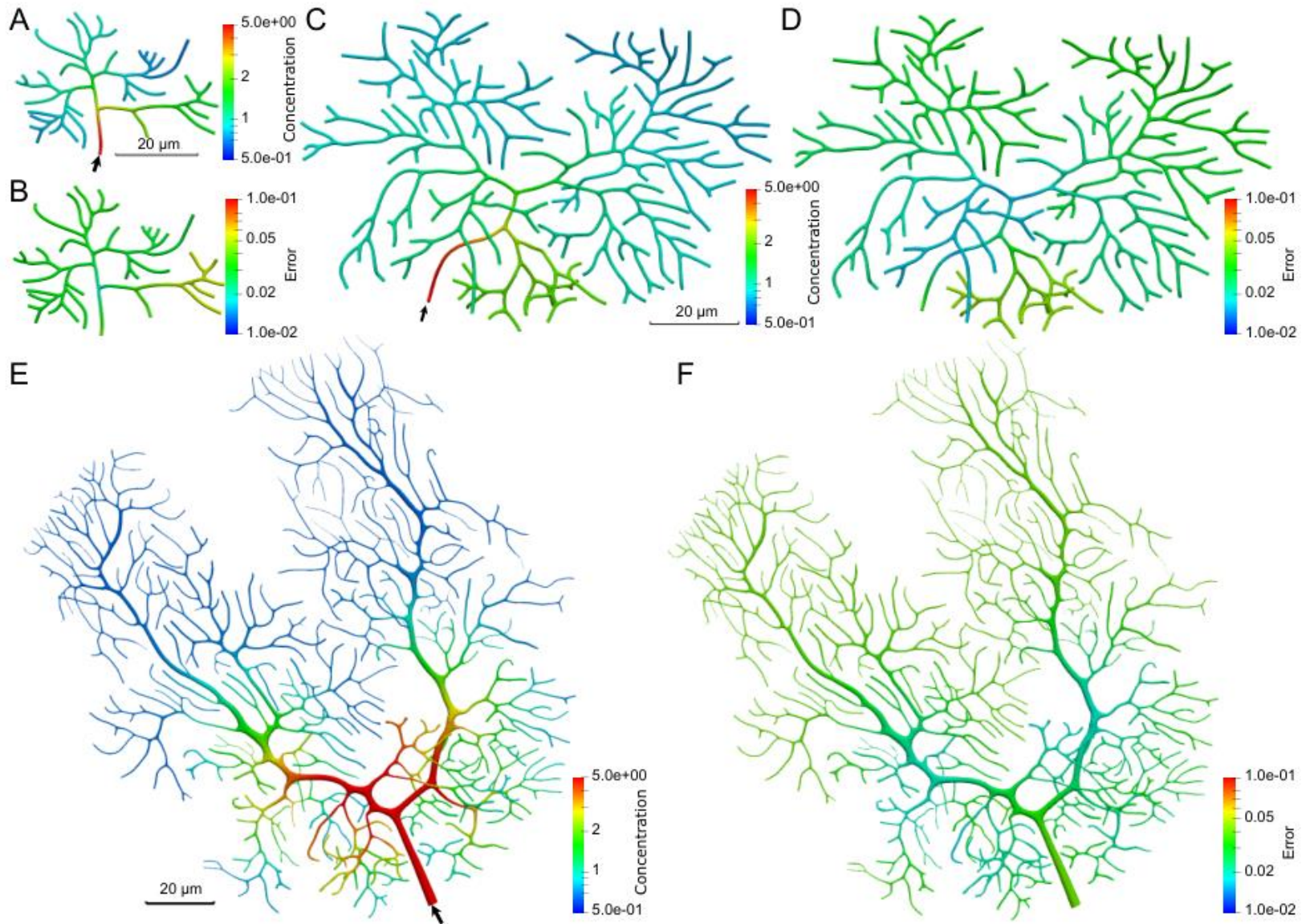


Figure: (A,B) NMO_54504; (C,D) NMO_54499; (E,F) NMO_00865.

Results - prediction in complex neuron trees

We summarize the details of the computation for each tree in the following table:

Table: Statistics of all tested complex neurite networks

Species	Model name	Mesh (vertices, elements)	Bifurcation number	IGA computation (nodes, time (mins))	GNN prediction time (mins)	Speedup ratio (IGA vs GNN)	GNN prediction MRE
Zebrafish	NMO_66731 (Fig. 3.4B)	(127,221, 112,500)	15	(8, 468)	1.6	293	6.7%
	NMO_66748 (Fig. 3.4D)	(282,150, 249,660)	35	(10, 672)	3.9	172	7.3%
	NMO_06846 (Fig. 3.5A)	(116,943, 101,880)	20	(8, 413)	2.1	197	7.2%
	NMO_06840 (Fig. 3.5B)	(280,434, 248,040)	35	(10, 705)	4.4	160	7.5%
Mouse	NMO_112145 (Fig. 3.5C)	(110,985, 98,460)	9	(8, 350)	1.2	291	7.4%
	NMO_32235 (Fig. 3.5H)	(96,714, 85,680)	9	(6, 320)	1.3	246	7.8%
	NMO_32280 (Fig. 3.5I)	(131,967, 117,000)	12	(8, 493)	1.5	329	8.1%
	NMO_54504 (Fig. 3.6A)	(116,943, 101,880)	32	(8, 436)	3.1	140	8.3%
	NMO_54499 (Fig. 3.6C)	(524,871 459,360)	127	(20, 759)	6.1	124	8.7%
	NMO_00865 (Fig. 3.6E)	(1,350,864, 1,179,900)	356	(40, 908)	7.1	127	9.1%

- Our GNN model provides high accurate prediction with all the prediction MRE below 9%.
- The average prediction MREs of zebrafish and mouse neurons are comparable with 7.18% and 8.23%.
- Our GNN model can achieve up to 330 times faster compared to IGA simulation.
- The model performs worse in longer branches or regions with a high density of bifurcations due to increasing complexity of the geometry.

Summary

- We develop a GNN-based deep learning model to study neuron transport pattern from simulation results.
- The model can tackle different neuron geometries with the use of GNN assembly model.
- The model can provide the spatiotemporal concentration prediction with MRE < 10% and over 100 times faster than the IGA simulation.

Modeling Material Transport Regulation and Traffic Jam In Neurons Using PDE- constrained Optimization

Background

- **Microtubules (MTs) swirls and induced axonal swelling in abnormal neuron**

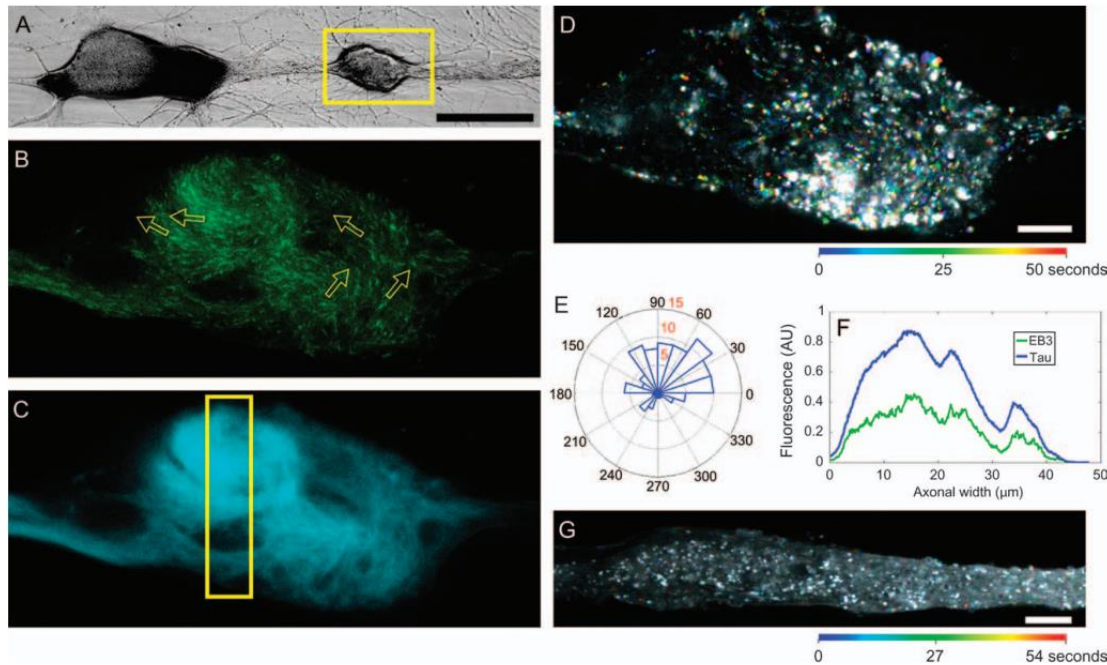


Fig. Formation of MT swirls underlies axonal swelling and transport defects in tau overexpressing neurons

- **Motivation: Though our IGA solver and GNN model can effectively simulate the transport process in complex neuron geometries, the motor-assisted transport model is too simple to simulate and explain the traffic jam phenomenon.**

- The tau-induced impairment of organelle transport is caused by polar reorientation of the MTs along the axon or their displacement to submembrane domains.
- Therefore, ‘traffic jams’ reflect the accumulation of organelles are observed at points of MT polar discontinuities or polar mismatching rather than because of MT depolymerization.

Modeling neuron material transport control using PDE constrained optimization

- Based on the motor-assisted transport model, we propose to use PDE-constrained optimization (PDE-CO) to model the traffic jam and the active regulation from neurons to control the transport process:

Minimizing the object function $J(n_{\pm}, v_{\pm}, f_{\pm}) = \frac{1}{2} \int_0^T \int_{\Omega} (v_{\pm}(\mathbf{x}, t) - V_{\pm}(\mathbf{x}))^2 d\Omega dt + \frac{\alpha}{2} \int_0^T \int_{\Omega} \left(\frac{\partial n_{\pm}(\mathbf{x}, t)}{\partial \mathbf{x}} \right)^2 d\Omega dt + \frac{\beta}{2} \int_0^T \int_{\Omega} f_{\pm}^2 d\Omega dt$

Such that

$$\frac{\partial n_0(\mathbf{x}, t)}{\partial t} = -(k_+ + k_-)n_0 + k'_+ l_+ n_+ + k'_- l_- n_-$$

$$\frac{\partial l_{\pm} n_{\pm}(\mathbf{x}, t)}{\partial t} + \mathbf{v}_{\pm} \frac{\partial l_{\pm} n_{\pm}(\mathbf{x}, t)}{\partial \mathbf{x}} = \frac{\partial}{\partial \mathbf{x}} \left(D_{\pm} \frac{\partial l_{\pm} n_{\pm}(\mathbf{x}, t)}{\partial \mathbf{x}} \right) + k_{\pm} n_0 - k'_{\pm} l_{\pm} n_{\pm}$$

$$\frac{\partial \mathbf{v}_{\pm}(\mathbf{x}, t)}{\partial t} + \mathbf{v}_{\pm} \frac{\partial \mathbf{v}_{\pm}(\mathbf{x}, t)}{\partial \mathbf{x}} = -\frac{\partial n_{\pm}(\mathbf{x}, t)}{\partial \mathbf{x}} + \frac{\partial}{\partial \mathbf{x}} \left(\mu \frac{\partial \mathbf{v}_{\pm}(\mathbf{x}, t)}{\partial \mathbf{x}} \right) + f_{\pm}$$

New terms added to model the traffic control mechanism

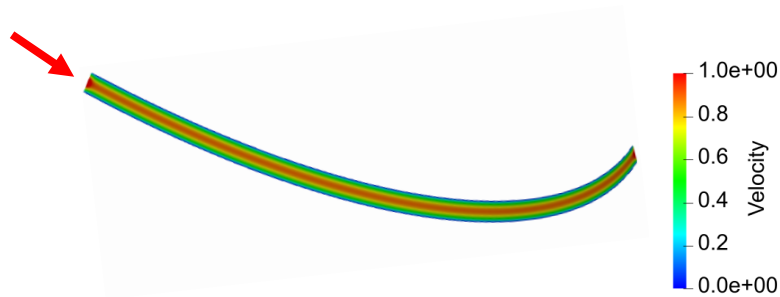
- $V_{\pm}(x)$ is the predefined velocity distribution to control velocity.
- α represents to what extent we want to optimize the transport process and avoid traffic jam.
- l_{\pm} represents the density of microtubules used for motor-assisted transport.
- f_{\pm} represents the control forces (or accelerations) that used to mediate the material traffic.

[1] A. Li, Y. J. Zhang. Modeling Intracellular Transport and Traffic Jam in 3D Neurons Using PDE-Constrained Optimization. *Special Issue of Journal of Mechanics on Recent Advances in IGA*, 38:44-59, 2022.

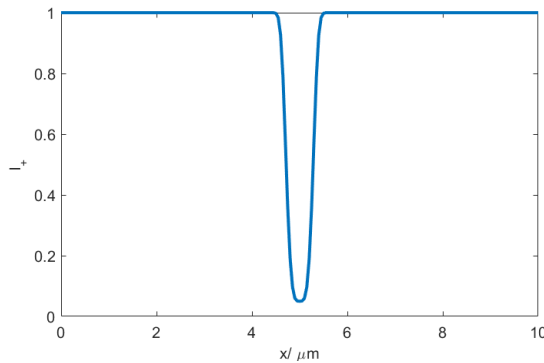
[2] A. Li, Y. J. Zhang. Modeling Material Transport Regulation and Traffic Jam in Neurons Using PDE-Constrained Optimization. *Scientific Reports*, 12:3902, 2022.

Result for 2D pipe geometry

- Desire velocity profile:



- l_+ distribution for introducing traffic jam



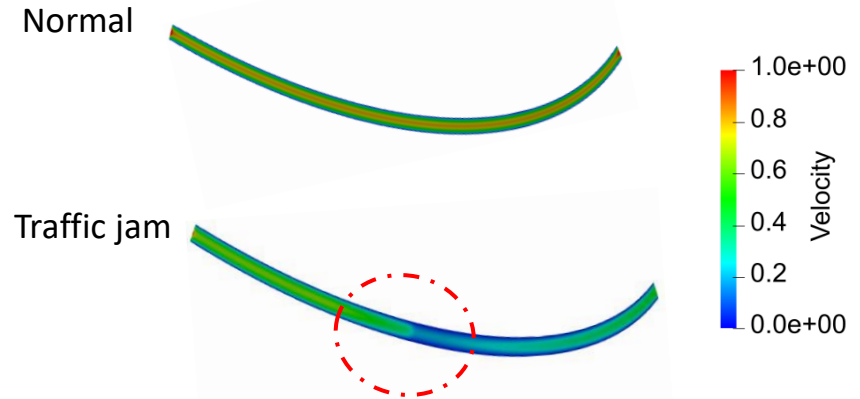
- Default Parameter settings:

$$D_+ = 0.1, k_+ = 1.0, k'_+ = 0.1, l_+ = 1.0, \\ \alpha = 1.0, \beta = 1.0$$

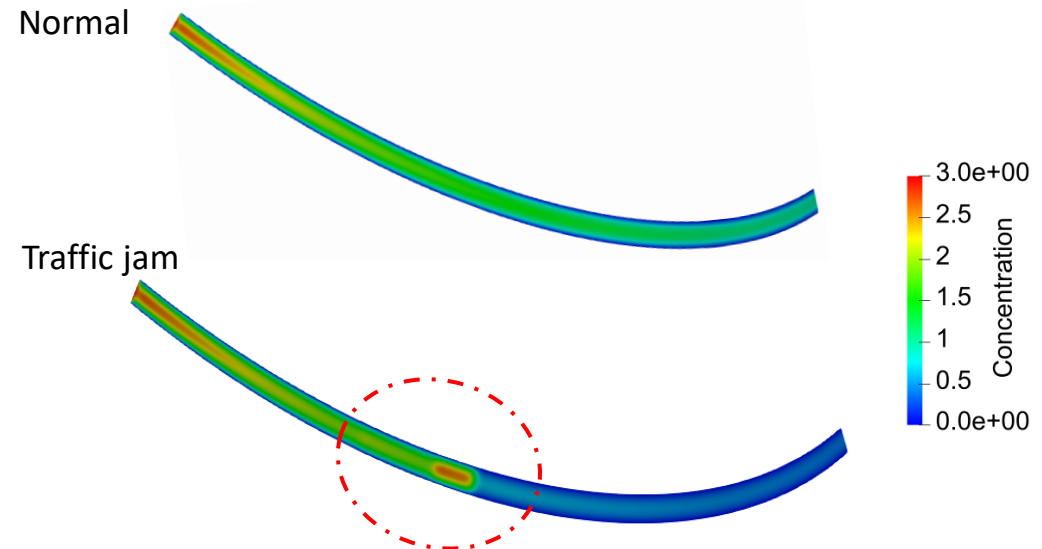
- Boundary conditions:

$$\text{Inlet: } n_0 = 1, n_+ = 2, n_- = 0, v_{+x} = 1.0, v_{+y} = 0$$

- Computed **velocity** profile:



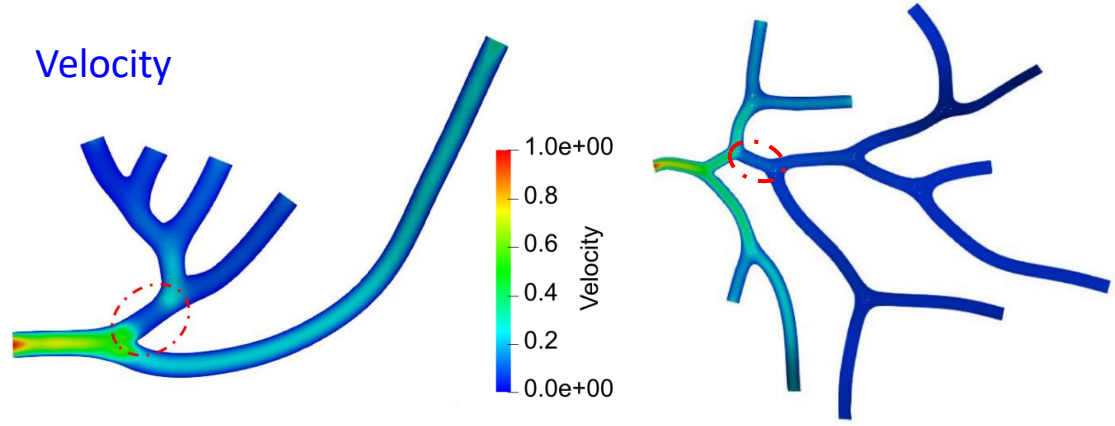
- Computed **concentration** profile and distribution along geometry centerline



Result for 2D neuron trees with reduced MTs

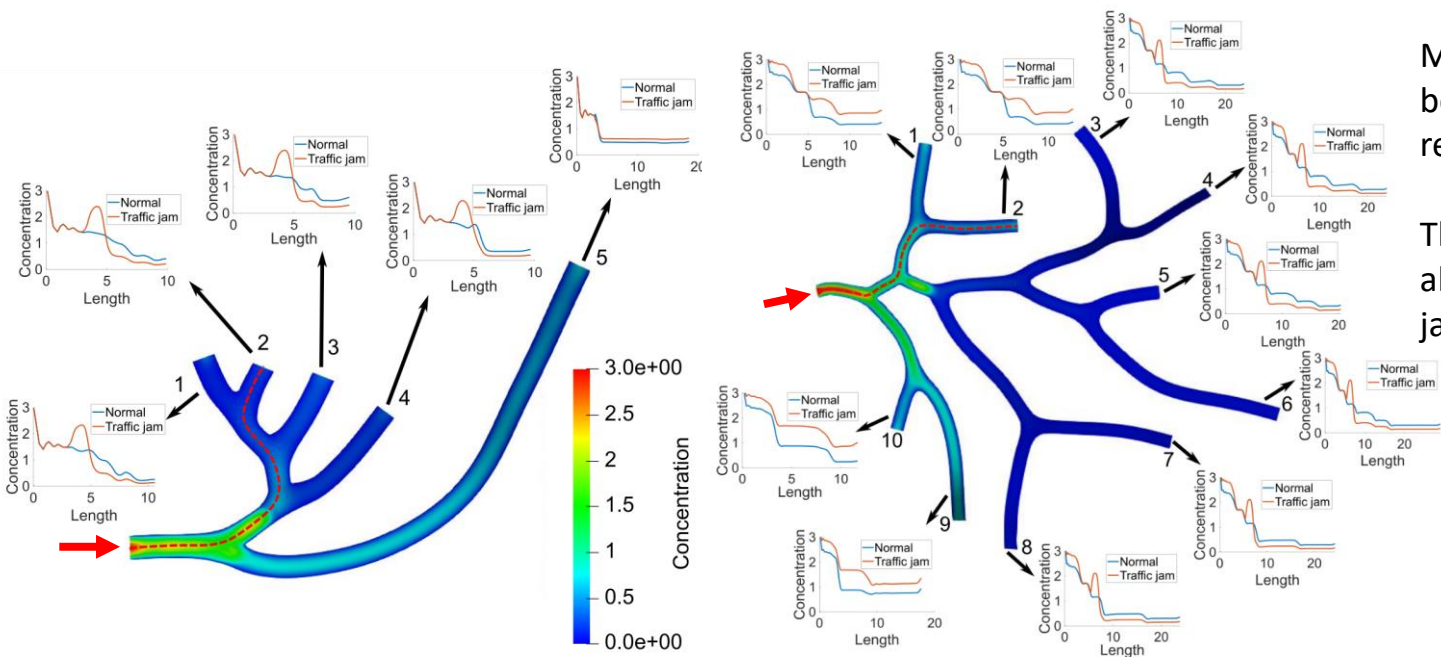
Reduce the number of MTs in the red circle region of two neuron trees

- Velocity



The decrease of velocity is observed in the traffic jam region

- Material concentration and the curve plot from the inlet to every outlet of the neuron tree



Material accumulation can be observed in the local region

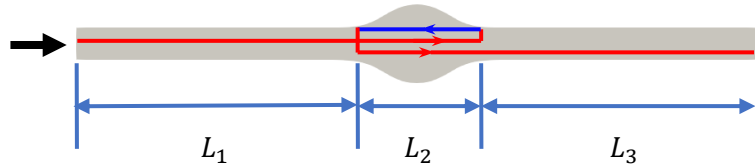
The outlet concentration is also affected by the traffic jam

NMO_54505

NMO_54499

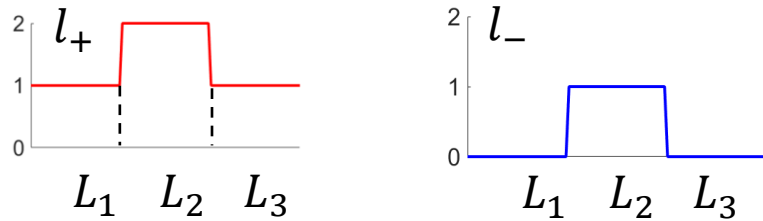
Result for 2D single pipe with swelling and MT swirls

- Simulation setting for MT swirls

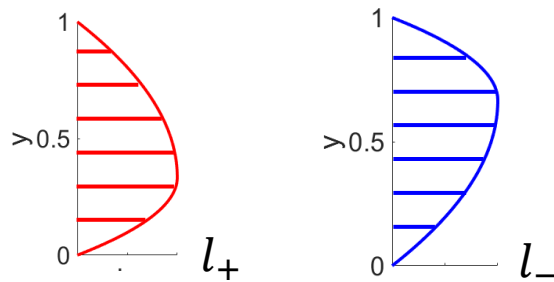


- l_{\pm} distribution for introducing traffic jam

Along centerline:



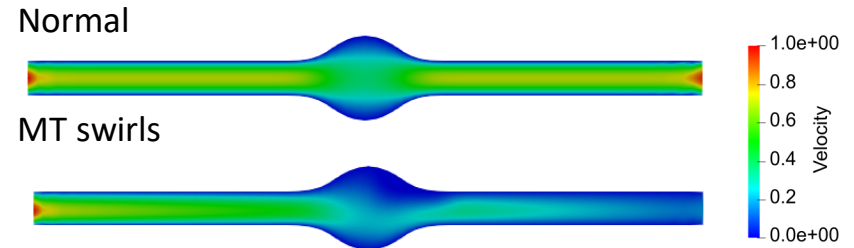
On cross-section:



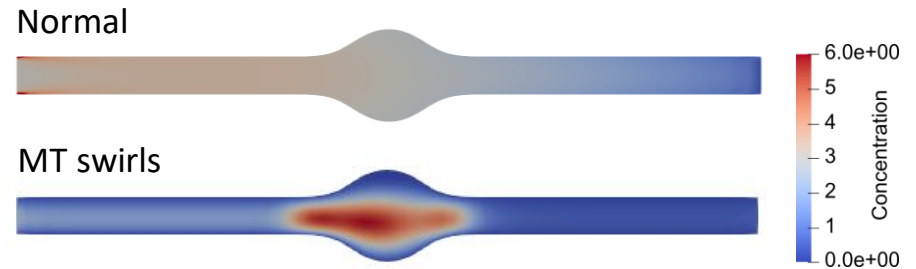
- Default Parameter settings:
 $D_+ = 0.1, k_+ = 1.0, k'_+ = 0.1, \alpha = 1.0, \beta = 1.0$

- Boundary conditions:
 Inlet: $n_0 = 1, n_+ = 2, n_- = 0, v_{+x} = 1.0, v_{+y} = 0$

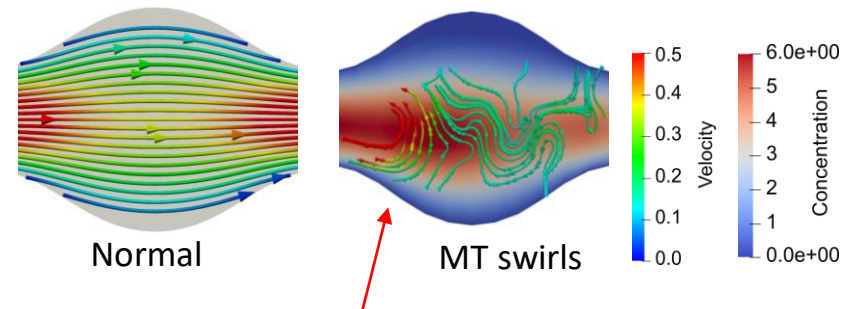
- Computed **velocity** profile



- Computed **concentration** profile



- Concentration + velocity streamline** at swollen region



Vortex pattern velocity streamline is observed at high concentration region

Simulation settings for modeling traffic jam in 3D

Three types of transport conditions:

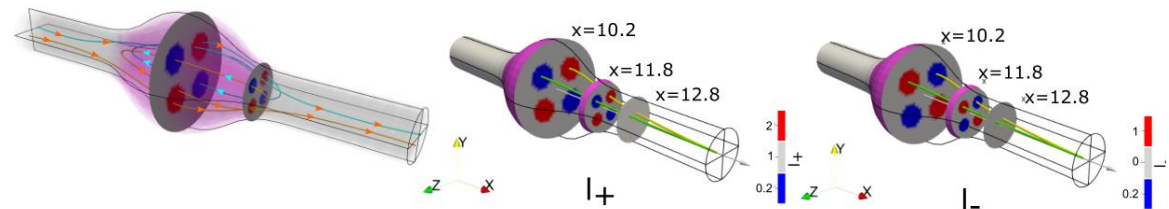
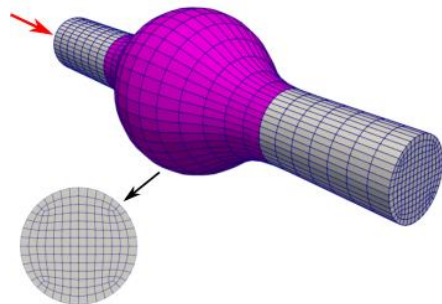
1. Normal transport: assuming a unidirectional transport with a unipolar MT system
2. Traffic jam caused by reduced number of MTs: decrease MT distribution in the traffic jam region and the definition of l_+ in a single pipe is

$$l_+(x) = 1 - 0.9 * \exp[-400(x - 0.5L)^4]$$

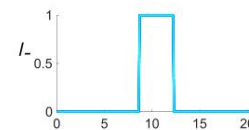
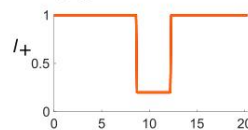
3. Traffic jam caused by MT swirls:

- The traffic jam is introduced at the swollen region (Pink color)
- The distribution of l_+ and l_- are set differently within the cross section of the swollen region. Red regions have MTs point to the outlet while the blue regions have MTs reverse back to the inlet direction. We have

$$\begin{cases} l_+ = 2.0, & l_- = 0.2 & \text{in red region,} \\ l_+ = 0.2, & l_- = 1.0 & \text{in blue region,} \\ l_+ = 1.0, & l_- = 0.0 & \text{otherwise.} \end{cases}$$



Along green curve



Along yellow curve

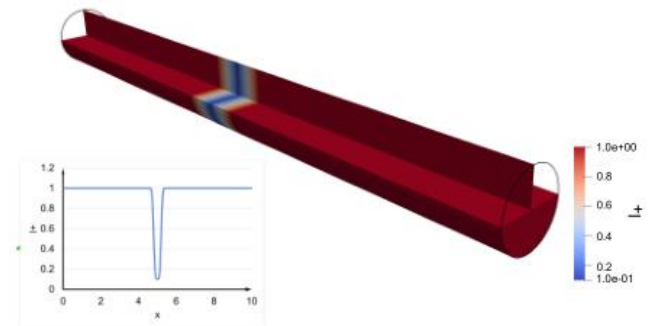
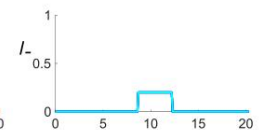
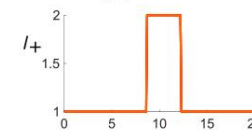
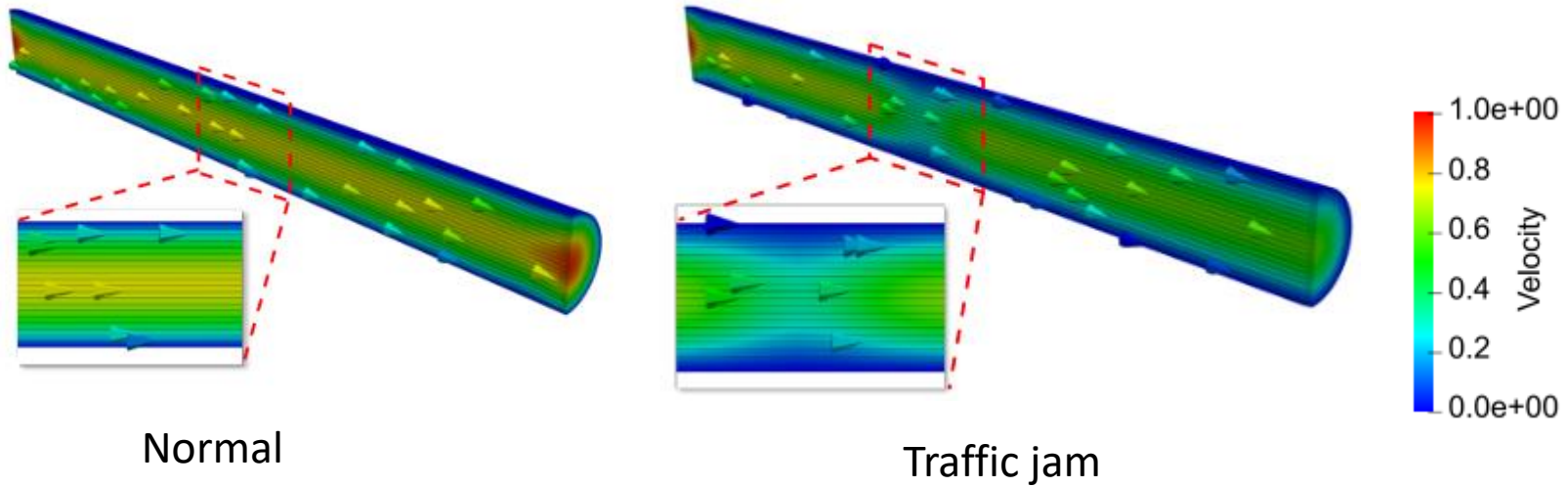


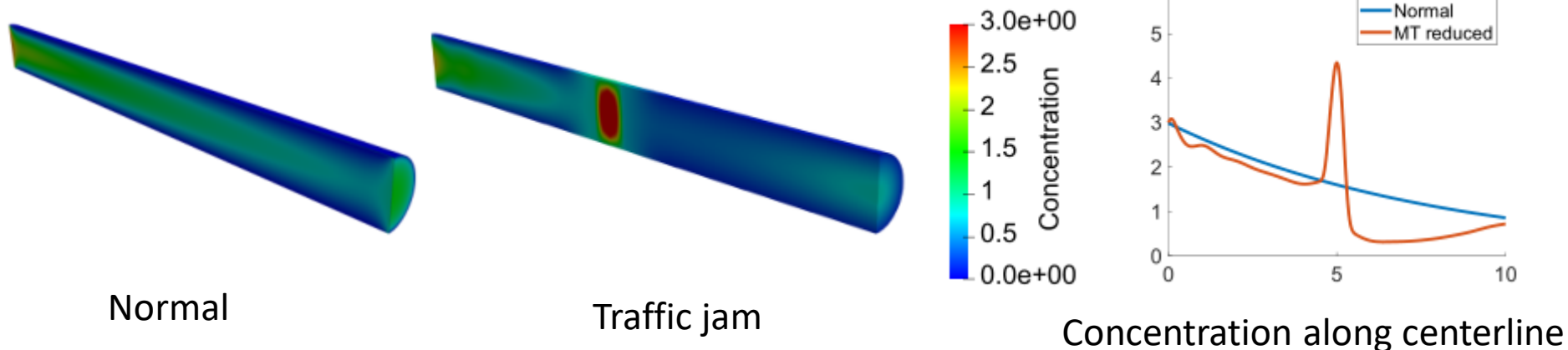
Figure 1: l_+ distribution along single pipe

Result for single pipe with reduced number of MTs

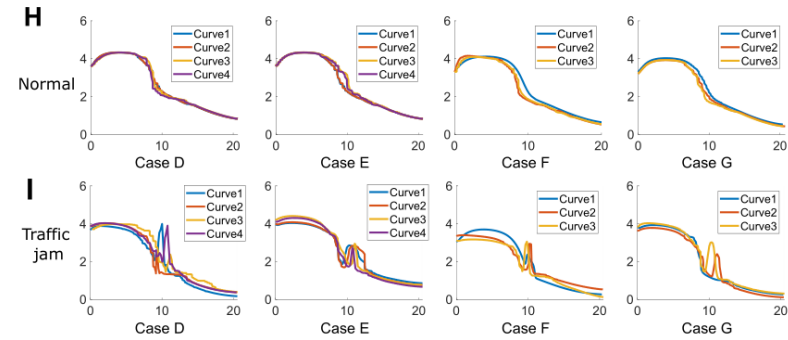
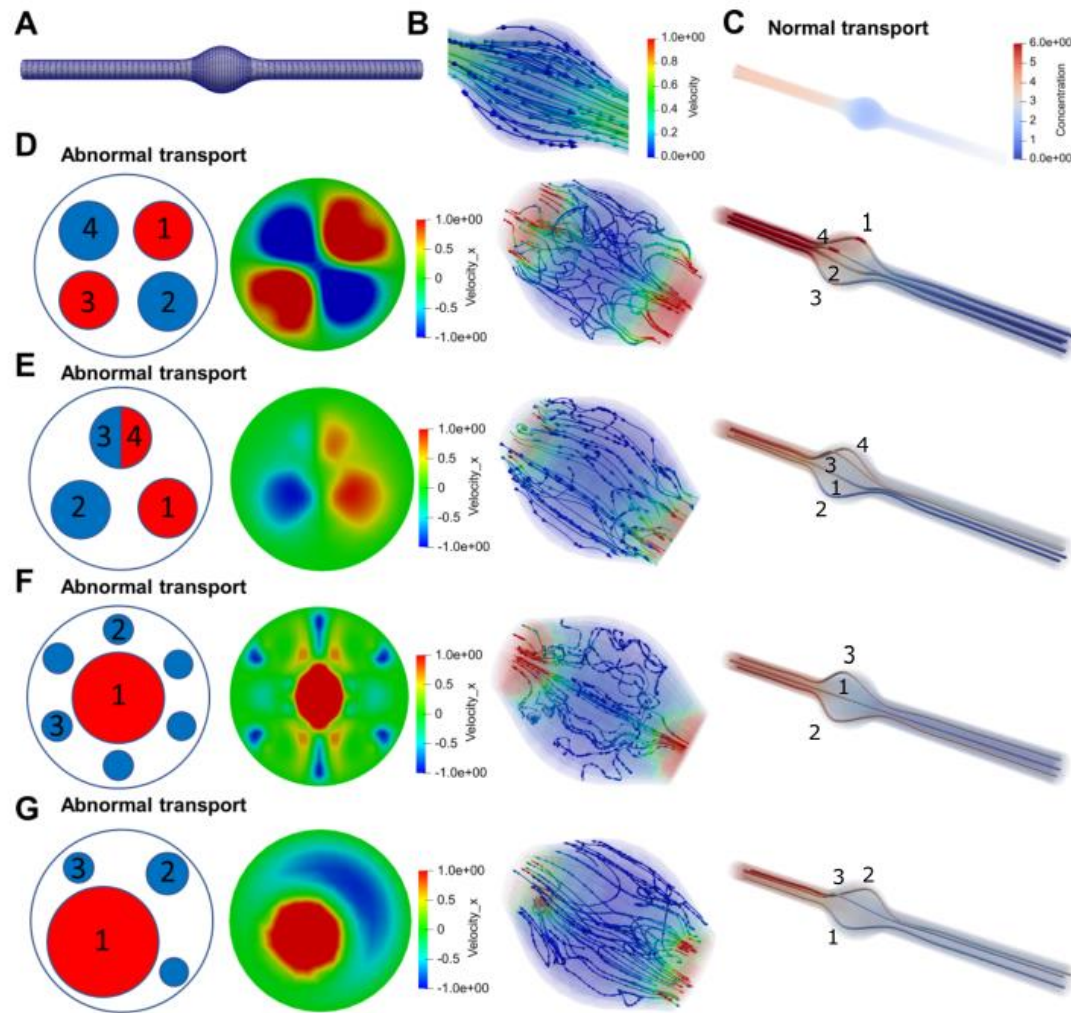
- Velocity



- Concentration



Result for single pipe with swelling and MT swirls



- We observe reversing and vortex pattern streamlines that caused by distribution of different direction MTs
- We find that the reversing streamline mainly occurs between the red and blue region, indicating the transport path of material is extended or even trapped in the local region.
- We find that the material flux is significantly decreased in all the traffic jam results compared with the normal transport.

	Fig. C Normal transport	Fig. D	Fig. E	Fig. F	Fig. G
Area ratio A_{red}/A_{blue}	-	1.0	1.0	1.5	2.1
Flux	0.9415	0.22418 (-75%)	0.2506 (-73%)	0.3804 (-58%)	0.4027 (-56%)

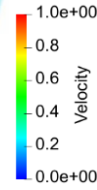
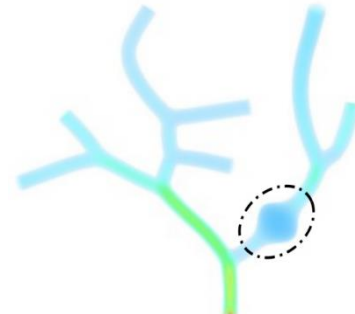
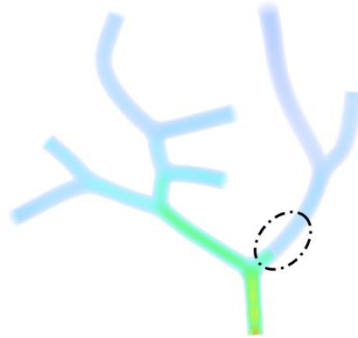
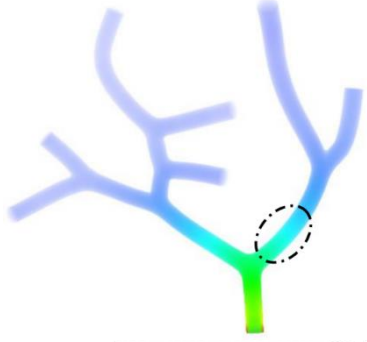
Modeling traffic jam in the neuron tree extracted from NMO_54499

Normal transport

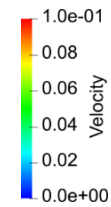
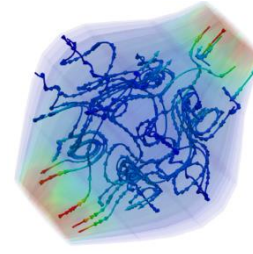
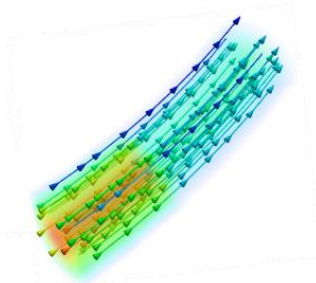
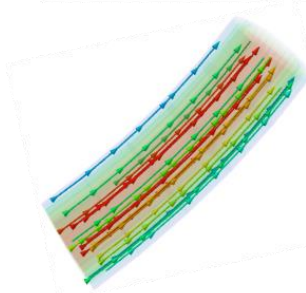
Traffic jam (Reduced MTs)

Traffic jam (MT swirls)

Velocity

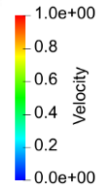
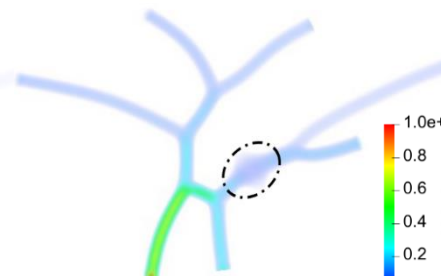
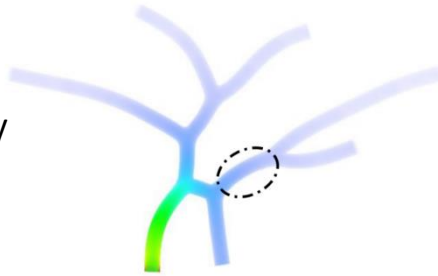


Local Streamline

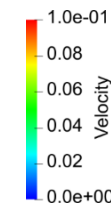
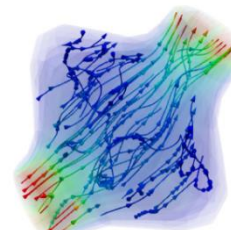
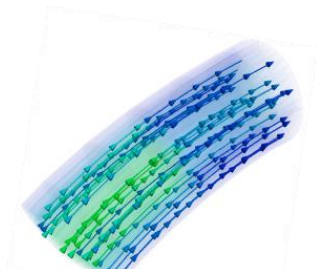
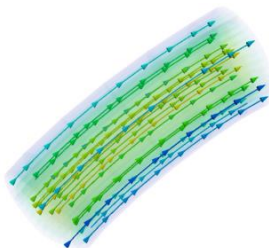


- A sudden decrease of velocity is observed in the traffic jam region.
- The reversing and vortex pattern streamlines are observed in the region with MT swirls

Velocity



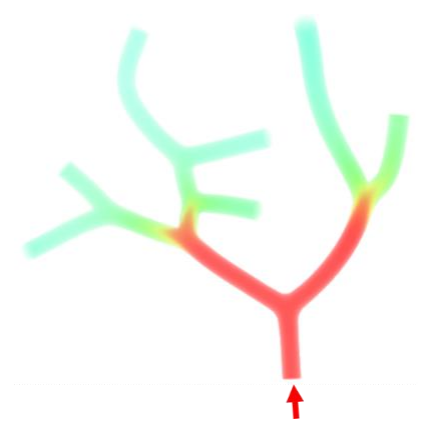
Local Streamline



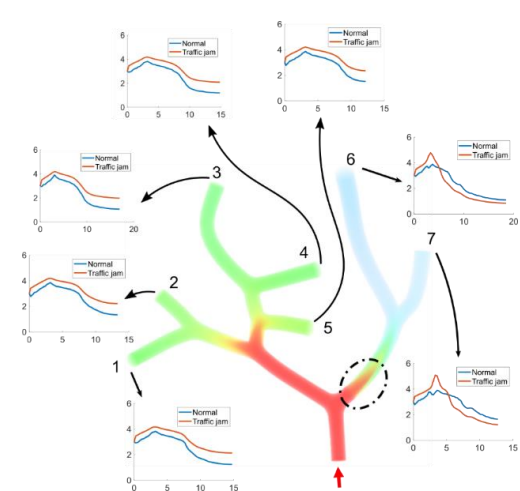
Modeling traffic jam in two neuron trees extracted from NMO_54499 - Concentration

Tree 1

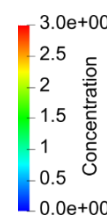
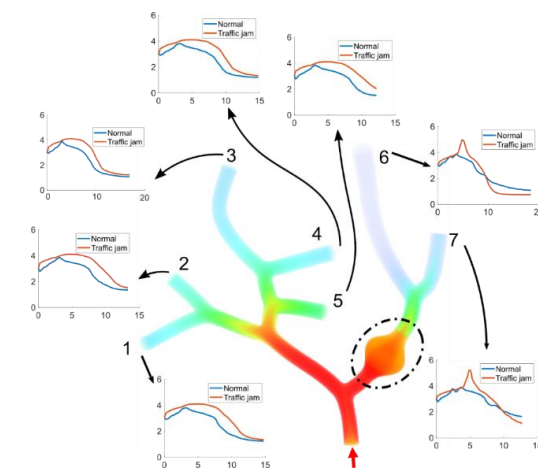
Normal transport



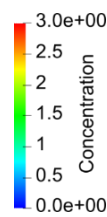
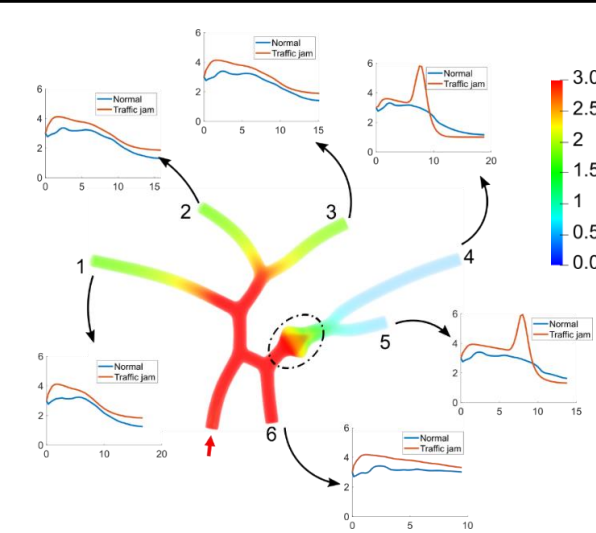
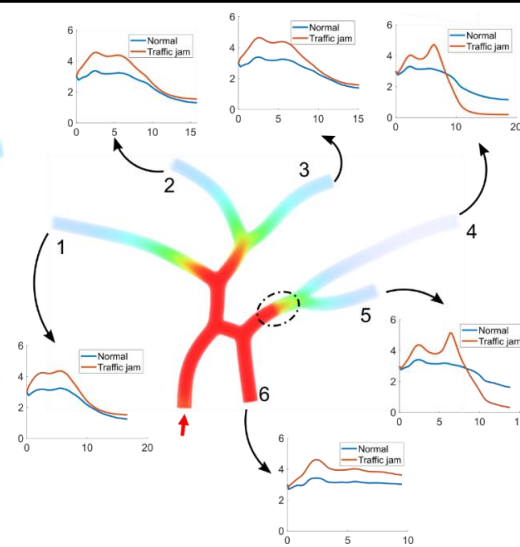
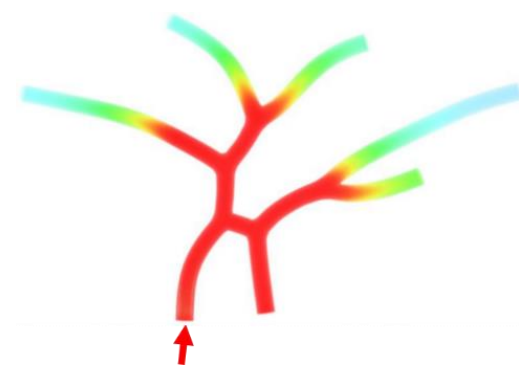
Traffic jam (Reduced MTs)



Traffic jam (MT swirls)



Tree 2



- The distribution plots from the inlet to each outlet show the material accumulation in the traffic jam region.
- The material concentration is reduced in the outlets downstream the traffic jam region.
- More materials are transported to the branches without traffic jam to mitigate the accumulation.

Summary

- The transport process is mediated by microtubules (MTs)

Our study shows that MTs have a major impact on the material transport velocity and further affect the material concentration distribution. The reduction of MTs in the local region can slow down the transport velocity and lead to traffic jam in this region.

- The simulation potentially explains the formation of traffic jam

Due to MT swirls, the streamline with vortex pattern is observed and it not only extends the transport distance but also traps the material in the local region, and therefore explains why high concentration region matches with the circular streamline pattern.

- An IGA-based optimization framework to study cellular process in neuron

The IGA optimization solver provides an efficient computation tool for studies of material transport regulation in complex neurite networks. The solver can also be extended to solve other PDE-CO models of cellular processes in complex neurite network geometry.

Conclusion

- We have developed an IGA-based platform for material transport simulation and tested the IGA solver within multiple complex and representative neurite networks.
- To address the high computational cost of the IGA solver, we have developed a GNN-based deep learning framework to learn from IGA simulation data and provide fast material concentration prediction.
- We have then developed a novel PDE-CO transport model to further study the traffic control mechanism and explain the traffic jam formation during the transport process.

Future work

- **Model improvement**

We need to improve the transport model to account for the effect of traffic jam on the effect on the deformation of neuron geometries. To address this limitation, we can couple the transport model with a structural model and solve a fluid-structure interaction problem to simulate the geometry deformation during traffic jam.

- **Model validation with biological experiments**

Biological experiments are necessary to validate our model. We need to derive more accurate parameter setting from the experiment and test our solver in complex geometry.

- **Application in studying other related biological process**

The material transport model can be used to study other related biological process such as neuron growth, which will help understand the neuron growth process and neurodegenerative diseases.

Publication

1. **A. Li**, Y. J. Zhang. Isogeometric Analysis-based Physics-Informed Graph Neural Network for Studying Traffic Jam in Neurons. *Under Review*, 2022.
2. **A. Li**, Y. J. Zhang. Modeling Intracellular Transport and Traffic Jam in 3D Neurons Using PDE-Constrained Optimization. *Special Issue of Journal of Mechanics on Recent Advances in IGA*, 38:44-59, 2022.
3. **A. Li**, Y. J. Zhang. Modeling Material Transport Regulation and Traffic Jam in Neurons Using PDE-Constrained Optimization. *Scientific Reports*, 12:3902, 2022.
4. **A. Li**, A. B. Farimani, Y. J. Zhang. Deep Learning of Material Transport in Complex Neurite Networks. *Scientific Reports*, 11:11280, 2021.
5. **A. Li**, R. Chen, A. B. Farimani, Y. J. Zhang. Reaction Diffusion System Prediction Based on Convolutional Neural Network. *Scientific Reports*, 10:3894, 2020.
6. **A. Li**, X. Chai, G. Yang, Y. J. Zhang. An Isogeometric Analysis Computational Platform for Material Transport Simulations in Complex Neurite Networks. *Molecular & Cellular Biomechanics*, 16(2):123-140, 2019.
7. X. Liang, **A. Li**, A. D. Rollett, Y. J. Zhang. An Isogeometric Analysis Based Topology Optimization Framework for Additive Manufacturing of 2D Cross-Flow Heat Exchangers. *Engineering with Computers*, under review, 2022.
8. Y. Yu, X. Wei, **A. Li**, J. G. Liu, J. He, Y. J. Zhang. HexGen and Hex2Spline: Polycube-Based Hexahedral Mesh Generation and Unstructured Spline Construction for Isogeometric Analysis Framework in LS-DYNA. *Springer INdAM Serie: Proceedings of INdAM Workshop "Geometric Challenges in Isogeometric Analysis."* Rome, Italy. Jan 27-31, 2020.
9. H. Casquero, X. Wei, D. Toshniwal, **A. Li**, T. J.R. Hughes, J. Kiendl, Y. J. Zhang. Seamless Integration of Design and Kirchhoff-Love Shell Analysis Using Analysis-Suitable Unstructured T-splines. *Computer Methods in Applied Mechanics and Engineering*, 360:112765, 2020.
10. X. Chai, D. Qian, Q. Ba, **A. Li**, Y. J. Zhang, G. Yang. Image-Based Measurement of Cargo Traffic Flow in Complex Neurite Networks. In *IEEE International Conference on Image Processing (pp.3290-3294)*, 2017

Thank you!